

Journal of Medical Genetics

Biallelic variants in Plexin B2 (*PLXNB2*) cause amelogenesis imperfecta, hearing loss and intellectual disability.

Journal:	<i>Journal of Medical Genetics</i>
Manuscript ID	jmg-2023-109728.R2
Article Type:	Original research
Date Submitted by the Author:	n/a
Complete List of Authors:	<p>Smith, Claire; University of Leeds Faculty of Medicine and Health, Institute of Medical Research, St James's University Hospital Laugel-Haushalter, Virginie; Université de Strasbourg, Institut de Génétique et de Biologie Moléculaire et Cellulaire (IGBMC), INSERM U1258, CRNS-UMR7104 Hany, Ummey; University of Leeds Faculty of Medicine and Health, Institute of Medical Research, St James's University Hospital Best, Sunayna; University of Leeds Faculty of Medicine and Health, Institute of Medical Research, St James's University Hospital; Leeds Teaching Hospitals NHS Trust, Yorkshire Regional Genetics Service Taylor, Rachel; Manchester University NHS Foundation Trust, Manchester Centre for Genomic Medicine, St Mary's Hospital; EMQN CIC Poulter, James; University of Leeds Faculty of Medicine and Health, Leeds Institute of Medical Research, St James's University Hospital Wortmann, Saskia; Paracelsus Medical University Salzburg, Department of Pediatrics, University Children's Hospital; Radboudumc, Amalia Children's Hospital Feichtinger, Rene; Paracelsus Medical University Salzburg, Department of Pediatrics, University Children's Hospital Mayr, Johannes; Paracelsus Medical University Salzburg, Department of Paediatrics, University Children's Hospital Al Bahlani, Suhaila; Government of Oman Ministry of Health, Dental & OMFS Clinic, Al Nahdha Hospital Nikolopoulos, Georgios; BSRC Alexander Fleming, Institute for Fundamental Biomedical Research Rigby, Alice; University of Leeds Faculty of Medicine and Health, Institute of Medical Research; University of Leeds Faculty of Medicine and Health, School of Dentistry Black, Graeme; University of Manchester Institute of Science and Technology Department of Biomolecular Science, Division of Evolution and Genomic Sciences, Manchester Academic Health Science Centre; Manchester University NHS Foundation Trust, Manchester Centre for Genomic Medicine, St Mary's Hospital Watson, Christopher; University of Leeds Faculty of Medicine and Health, Institute of Medical Research, St James's University Hospital; Leeds Teaching Hospitals NHS Trust, North East and Yorkshire Genomic Laboratory Hub, Central Lab, St James's University Hospital Mansour, Sahar; University of London, Lymphovascular Research Unit, Molecular and Clinical Sciences Research Institute, St George's Hospital;</p>

1
2
3
4
5
6
7
8
9
10
11
12
13
14
15
16
17
18
19
20
21
22
23
24
25
26
27
28
29
30
31
32
33
34
35
36
37
38
39
40
41
42
43
44
45
46
47
48
49
50
51
52
53
54
55
56
57
58
59
60

	<p>St George's University Hospitals NHS Foundation Trust, SW Thames Regional Centre for Genomics Inglehearn, Chris; University of Leeds Faculty of Medicine and Health, Institute of Medical Research, St James's University Hospital Mighell, Alan; University of Leeds Faculty of Medicine and Health, School of Dentistry Bloch-Zupan, Agnès; University of Strasbourg, Institut de Génétique et de Biologie Moléculaire et Cellulaire (IGBMC), INSERM U1258, CNRS-UMR7104; University of Strasbourg Faculty of Medicine</p>
<p>Keywords:</p>	<p>Dentistry, Dentistry, Genetic Research, Genetics, Genetics, Medical</p>





I, the Submitting Author has the right to grant and does grant on behalf of all authors of the Work (as defined in the below author licence), an exclusive licence and/or a non-exclusive licence for contributions from authors who are: i) UK Crown employees; ii) where BMJ has agreed a CC-BY licence shall apply, and/or iii) in accordance with the terms applicable for US Federal Government officers or employees acting as part of their official duties; on a worldwide, perpetual, irrevocable, royalty-free basis to BMJ Publishing Group Ltd ("BMJ") its licensees and where the relevant Journal is co-owned by BMJ to the co-owners of the Journal, to publish the Work in this journal and any other BMJ products and to exploit all rights, as set out in our [licence](#).

The Submitting Author accepts and understands that any supply made under these terms is made by BMJ to the Submitting Author unless you are acting as an employee on behalf of your employer or a postgraduate student of an affiliated institution which is paying any applicable article publishing charge ("APC") for Open Access articles. Where the Submitting Author wishes to make the Work available on an Open Access basis (and intends to pay the relevant APC), the terms of reuse of such Open Access shall be governed by a Creative Commons licence – details of these licences and which [Creative Commons](#) licence will apply to this Work are set out in our licence referred to above.

Other than as permitted in any relevant BMJ Author's Self Archiving Policies, I confirm this Work has not been accepted for publication elsewhere, is not being considered for publication elsewhere and does not duplicate material already published. I confirm all authors consent to publication of this Work and authorise the granting of this licence.

1
2
3 **Biallelic variants in Plexin B2 (*PLXNB2*) cause amelogenesis imperfecta, hearing loss**
4 **and intellectual disability.**
5
6

7
8 Claire E L Smith^{1*}, Virginie Laugel-Haushalter^{2*}, Ummey Hany¹, Sunayna Best^{1,3}, Rachel L
9 Taylor^{4,5,6}, James A. Poulter¹, The UK Inherited Retinal Disease Consortium, Genomics
10 England Research Consortium, Saskia B Wortmann^{7,8}, René G Feichtinger⁷, Johannes A
11 Mayr⁷, Suhaila Al Bahlani⁹, Georgios Nikolopoulos¹⁰, Alice Rigby^{1,11}, Graeme C Black^{4,5},
12 Christopher M. Watson^{1,12}, Sahar Mansour^{13,14}, Chris F Inglehearn¹, Alan J Mighell^{11*} and
13 Agnès Bloch-Zupan^{2,15,16*}
14
15
16
17
18
19
20
21
22
23

24 ¹Leeds Institute of Medical Research, St James's University Hospital, University of Leeds,
25 Beckett Street, Leeds. LS9 7TF. UK.

26
27
28 ² Institut de Génétique et de Biologie Moléculaire et Cellulaire (IGBMC), INSERM U1258,
29 CNRS-UMR7104, Université de Strasbourg, Illkirch, France.

30
31
32
33 ³Yorkshire Regional Genetics Service, Leeds Teaching Hospitals NHS Trust, Leeds. LS7
34 4SA. UK.

35
36
37 ⁴Division of Evolution and Genomic Sciences, Manchester Academic Health Science Centre,
38 Faculty of Biology, Medicine and Health, School of Biological Sciences, University of
39 Manchester, Manchester, M13 9NT. UK.

40
41
42
43
44 ⁵Manchester Centre for Genomic Medicine, St. Mary's Hospital, Manchester University NHS
45 Foundation Trust, Manchester. M13 9WL. UK.

46
47
48 ⁶EMQN CIC, Pencroft Way, Manchester Science Park, Manchester. M15 6SE. UK.

49
50
51
52 ⁷University Children's Hospital, Salzburger Landeskliniken (SALK) and Paracelsus Medical
53 University (PMU), Müllner Hauptstrasse 48, 5020 Salzburg, Austria.

54
55
56 ⁸Amalia Children's Hospital, Radboud University Medical Center, Geert Grooteplein Zuid
57 10, 6525 GA Nijmegen, the Netherlands.
58
59
60

1
2
3⁹Dental & O.M.F.S Clinic, Al Nahdha Hospital, Ministry of Health, Muscat. HGQJ+GV6.
4
5
6
7
8
9
10
11
12
13
14
15
16
17
18
19
20
21
22
23
24
25
26
27
28
29
30
31
32
33
34
35
36
37
38
39
40
41
42
43
44
45
46
47
48
49
50
51
52
53
54
55
56
57
58
59
60

Oman.

¹⁰Institute for Fundamental Biomedical Research, BSRC Alexander Fleming, 16672 Vari, Attica, Greece.

¹¹School of Dentistry, University of Leeds. LS2 9JT. UK.

¹²North East and Yorkshire Genomic Laboratory Hub, Central Lab, St. James's University Hospital, Leeds. LS9 7TF. UK.

¹³Lymphovascular Research Unit, Molecular and Clinical Sciences Research Institute, University of London St George's, London. SW17 0QT. UK.

¹⁴SW Thames Regional Centre for Genomics, St George's University Hospitals NHS Foundation Trust, London. SW17 0QT. UK.

¹⁵Faculté de Chirurgie Dentaire, Université de Strasbourg, 8 Rue Sainte Elisabeth, F-67000 Strasbourg, France.

¹⁶Centre de référence des maladies rares orales et dentaires O-Rares, Filière Santé Maladies rares TETE COU, European Reference Network CRANIO, Pôle de Médecine et Chirurgie Bucco-dentaires, Hôpital Civil, Hôpitaux Universitaires de Strasbourg (HUS), 1 place l'hôpital, 67000 Strasbourg, France.

* These authors contributed equally to the study.

Correspondence to:

Dr Claire E L Smith email C.E.L.Smith@leeds.ac.uk

Telephone (+44) 113 343 8445

Keywords: Semaphorins; amelogenesis; amelogenesis imperfecta; sensorineural hearing loss; intellectual disability; retinal dystrophies, lymphedema

Abstract

Background:

Plexins are large transmembrane receptors for the semaphorin family of signalling proteins. Semaphorin-plexin signalling controls cellular interactions that are critical during development as well as in adult life stages. Nine plexin genes have been identified in humans, but despite the apparent importance of plexins in development, only biallelic *PLXND1* and *PLXNA1* variants have so far been associated with Mendelian genetic disease.

Methods:

Eight individuals from six families presented with a recessively inherited variable clinical condition, with core features of amelogenesis imperfecta (AI) and sensorineural hearing loss (SNHL), with variable intellectual disability. Probandes were investigated by exome or genome sequencing. Common variants and those unlikely to affect function were excluded. Variants consistent with autosomal recessive inheritance were prioritised. Variant segregation analysis was performed by Sanger sequencing. RNA expression analysis was conducted in C57Bl6 mice.

Results:

Rare biallelic pathogenic variants in plexin B2 (*PLXNB2*), a large transmembrane semaphorin receptor protein, were found to segregate with disease in all six families. The variants identified include missense, nonsense, splicing changes and a multi-exon deletion. *Plxnb2* expression was detected in differentiating ameloblasts.

Conclusion:

1
2
3 We identify rare biallelic pathogenic variants in *PLXNB2* as a cause of a new autosomal
4 recessive, phenotypically diverse syndrome with AI and SNHL as core features. Intellectual
5 disability, ocular disease, ear developmental abnormalities and lymphoedema were also
6 present in multiple cases. The variable syndromic human phenotype overlaps with that seen
7 in *Plxnb2* knockout mice, and, together with the rarity of human *PLXNB2* variants, may
8 explain why pathogenic variants in *PLXNB2* have not been reported previously.
9
10
11
12
13
14
15
16
17
18

19 **What is already known on this topic**

20
21 Plexins are large transmembrane proteins that act as receptors for the semaphorin family of
22 signalling proteins. Semaphorin-plexin signalling controls cellular interactions that are
23 critical during development as well as in adult life stages. Nine plexin genes have been
24 identified in humans, but despite the apparent importance of plexins in development, only
25 biallelic *PLXND1* and *PLXNA1* variants have so far been associated with Mendelian genetic
26 disease.
27
28
29
30
31
32
33
34

35 **What this study adds**

36
37 We identify rare biallelic pathogenic variants in *PLXNB2* as a cause of a new autosomal
38 recessive, phenotypically diverse syndrome with amelogenesis imperfecta and sensorineural
39 hearing loss as core features. Intellectual disability, ocular disease, ear developmental
40 abnormalities and lymphoedema were also present in multiple cases. The variable syndromic
41 human phenotype overlaps with that seen in *Plxnb2* knockout mice, and, together with the
42 rarity of human *PLXNB2* variants, may explain why pathogenic variants in *PLXNB2* have not
43 been reported previously.
44
45
46
47
48
49
50
51
52
53

54 **How this study might affect research, practice or policy**

55
56 Individuals presenting with amelogenesis imperfecta and sensorineural hearing loss should be
57 screened for mutations in *PLXNB2* and tested for other features of the syndrome. *PLXNB2*
58
59
60

1
2
3 should be added to amelogenesis imperfecta, deafness and intellectual disability gene panels
4
5 to improve mutation detection rates. Affected families should receive appropriate genetic
6
7 counselling.
8
9
10
11
12
13
14
15
16
17
18
19
20
21
22
23
24
25
26
27
28
29
30
31
32
33
34
35
36
37
38
39
40
41
42
43
44
45
46
47
48
49
50
51
52
53
54
55
56
57
58
59
60

Confidential: For Review Only

Introduction

Development is a cascade of highly dynamic, time-critical, complex processes involving many signalling molecules and receptors that act to regulate cell proliferation, migration, adhesion and differentiation. This results in the formation of complex tissues, which further organise to effect organogenesis. Plexins are large transmembrane proteins that act as receptors for the semaphorin family of signalling proteins. Semaphorin-plexin signalling controls cellular interactions that are critical during development as well as in adult life stages (reviewed by Peralá et al. 2012).[1] Semaphorin signalling modulates changes to both actin and microtubule organisation and therefore to the overall cytoskeleton, cell morphology, cell adhesion and cell motility (reviewed in Alto & Terman[2]).

The plexin gene family was originally identified in humans, and members were grouped according to the domain structure of the encoded proteins.[3, 4] Nine genes have been identified in both humans and mice, with class A plexins consisting of 4 genes (A1-A4), class B of three (B1-B3) and classes C (C1) and D (D1) of one each.[1, 4] Plexin family members share a common structure, with extracellular and intracellular portions. The extracellular portions contain a sema domain that binds with semaphorin ligands to activate signalling, as well as two or three PSI (plexin, semaphorin and integrin) domains and two or three glycine-proline rich IPT (immunoglobulin, plexin and transcription factor) domains. The intracellular portions are highly conserved[5] and contain two R-Ras GAP motifs and one set of Plexin Rho-GTPase Association Motifs (PRAMs).

Class B plexins have an additional intracellular C-terminal PDZ interaction domain[6] and an extracellular cleavage site for proprotein convertases.[1] Plexin B2 (PLXNB2) participates in axonal guidance and cell migration.[7] It is expressed widely but it also demonstrates a specific temporospatial pattern of expression throughout development, and its expression is

1
2
3 distinct from that of other plexins, suggesting non-redundancy.[8] RNA transcripts are
4 detectable in mice from early fetal stages to adulthood within the brain.[9] In situ
5 hybridisation in E14 mouse embryos revealed high expression within several regions of the
6 central nervous system, including many regions of the brain and retina.[8] Expression was
7 also high in the developing tooth bud, oral epithelium and in cartilage, with lower expression
8 also detected in the cochlea, lung, kidney, epidermis and intestine.[8] The exact role of
9 PLXNB2 in tooth development is currently unknown, but semaphorins and plexin B1 have
10 been found to be important for innervation of tooth buds[10] and for dental stem cell
11 migration ex vivo.[11]

12
13
14
15
16
17
18
19
20
21
22
23
24 *Plxnb2* knockout mice (*Plxnb2*^{-/-}) vary in phenotype, depending upon their genetic
25 background. *Plxnb2*^{-/-} mice produced on inbred backgrounds did not survive gestation.[12,
26 13] The majority developed exencephaly, reflecting the importance of plexin B2 activity for
27 neural tube closure and potentially also its influence on the actin cytoskeleton. Other defects
28 noted included abnormal development of the dentate gyrus, defects in cerebellar foliation and
29 lamination, retarded development of the olfactory bulb and impaired neuronal proliferation.
30 In contrast, when the same pathogenic variant was introduced into outbred CD1 mice, neural
31 tube closure defects were less common, and after 4 generations, around 30% of *Plxnb2*^{-/-}
32 mice were viable and fertile. Despite the knockout mice having no obvious behavioural or
33 motor defects, their cerebella were smaller and major brain foliation defects were still
34 present.[12] Heterozygous *Plxnb2*^{+/-} mice had no apparent abnormalities.

35
36
37
38
39
40
41
42
43
44
45
46
47
48
49
50 Human *PLXNB2* variants (MIM*604293) and aberrant PLXNB2 expression have been
51 associated with lung cancer,[14, 15] acute myeloid leukaemia,[16] amyotrophic lateral
52 sclerosis,[17] glioblastoma,[18] autism spectrum disorders with regression,[19] psoriasis,[20]
53 and first trimester euploid miscarriage.[21] In contrast, despite the apparent importance of
54 plexins in development, only biallelic *PLXND1* (MIM*620282) and *PLXNA1* (MIM*601055)
55
56
57
58
59
60

1
2
3 variants have so far been associated with Mendelian genetic disease in humans. *PLXND1*
4
5 variants cause multiple types of congenital heart defects (MIM#620294).[22] *PLXNA1*
6
7 variants cause Dworschak-Punetha neurodevelopmental syndrome which includes speech
8
9 regression, autistic features and hyperactivity, variable sensorineural hearing loss (SNHL)
10
11 and ocular, brain, facial and skin abnormalities (MIM#619955).[23] The same authors also
12
13 suggested that pathogenic variants in other plexins may be embryonic lethal or may cause a
14
15 range of phenotypes that have not yet been recognised as part of one syndrome.[23]
16
17
18

19
20 Here we describe six families with probands carrying rare biallelic *PLXNB2* variants. Affected
21
22 individuals manifest a complex, variable syndromic phenotype, the core features of which
23
24 appear to be SNHL and amelogenesis imperfecta (AI), with intellectual disability also present
25
26 in most cases.
27
28
29
30
31
32
33
34
35
36
37
38
39
40
41
42
43
44
45
46
47
48
49
50
51
52
53
54
55
56
57
58
59
60

Materials and Methods

Patients

Affected individuals and family members were recruited in accordance with the principles outlined by the declaration of Helsinki, with local ethical approval (REC 13/YH/0028).

Clinical evaluation captured disease features as part of routine patient care. Genomic DNA was obtained from venous blood samples using a salt-based extraction protocol, or from saliva using Oragene DNA Sample Collection kits (DNA Genotek, Ottawa, ON, Canada) as detailed in the manufacturer's instructions.

Sequencing and analysis

Individuals were recruited and genomic DNA was subjected to SNP genotyping, exome or genome sequencing at different institutions. Sequencing and analysis methods for each family can be found in the Supplementary materials and methods. In summary, variants identified in next generation short-read sequencing data were filtered to exclude all changes other than missense, frameshift or stop variants, exonic insertion/deletions or variants located at splice consensus sites (up to 8 bp within introns or 3 bp within exons away from splice junctions). Synonymous variants outside of the splice region were discarded. Variants in the Genome Aggregation Database (gnomAD) (v2.2.1)[24] were excluded if present at a global minor allele frequency of 1% or higher. Variants were also filtered based on the mode of inheritance. In families known to be consanguineous, homozygous variants were prioritised. Population specific high frequency variants and platform artefacts were excluded by removing variants also present in exomes of individuals of the same ethnicity without dental disease that had been sequenced using the same reagents and platform. Splicing prediction analysis was carried out using NetGene2 (v2.4.2)[25] and Splice AI.[26] CADD v1.6.[27]

1
2
3 REVEL,[28] Polyphen-2 (HumVar model)[29] and SIFT[30] were used to assess each
4 variant's potential to be disease causing. Copy number variants were identified using
5 ExomeDepth (v1.0.0).[31] Variants were confirmed and segregation analysis was performed
6 for all available family members by Sanger sequencing. Primer sequences used are shown
7 in Supplementary Table 1. Genomic coordinates are based on the GRCh37 human reference
8 genome, the reference gene sequence used for *PLXNB2* is MANE Select transcript
9 NM_012401.4 (ENST00000359337.9) and protein variant nomenclature for PLXNB2 is
10 based on RefSeq protein NP_036533.2 (ENSP00000352288.4). The corresponding references
11 used for *CRYBB3* are MANE Select transcript NM_004076.5 (ENST00000215855.7) and for
12 *CRYBB3* RefSeq protein NP_004067.1 (ENSP00000215855.2). All variants identified as
13 part of this study were uploaded to ClinVar: SCV002822954 - SCV002822961. *In silico*
14 modelling of the effect of the variants on the PLXNB2 protein tertiary structure was
15 completed using iTASSER MTD[32] using the default parameters. The protein structures
16 were visualised with UCSF Chimera.[33]

38 **Mouse tissue preparation**

39 All animals were maintained in accordance with the French Ministry of Agriculture
40 guidelines for the use of laboratory animals under study SC67-218-37- IGBMC and
41 APAFIS#3957-2016020516359388v1 and in accordance with the NIH guidelines provided in
42 the Guide for the Care and Use of Laboratory Animals. All methods and experimental
43 procedures were reviewed and approved by an institutional safety committee.

44 Mouse embryos/fetuses were collected at E14.5, E16.5, E19.5 or on the day of birth and
45 analyzed as detailed in supplementary materials and methods.

Results

Initially we recruited two consanguineous families, one Turkish (Family 1) and one Omani (Family 2) (Figure 1). In Family 1, two male double first cousins have bilateral SNHL, intellectual disability, AI and severe myopia (Supplementary Figure 1). In addition to the shared phenotype, one (II:3) also has bilateral cataracts and the other (II:6) has unilateral renal agenesis and pyloric stenosis. Analysis of GeneChip® Human Mapping 250K *Nsp* SNP data from affected individuals II:3 and II:6 showed two homozygous regions encompassing chr7:34,080,354-41,760,000 and chr22:49,714,781-51,1756,26. Exome sequencing of II:3 and II:6 revealed a shared homozygous variant in *PLXNB2* within the region on chromosome 22, c.2413A>T, p.(Ile805Phe) (Table 1) which segregates with disease in the family (Supplementary Figure 2). It affects the extracellular portion of the protein, specifically the first cell surface receptor IPT domain and is predicted to be damaging by all pathogenicity prediction software tested (Supplementary Table 2). The residue affected is highly conserved (Supplementary Figure 3) and the variant is absent from gnomAD. Individual II:3 was also found to carry variant c.388G>A, p.(Glu130Lys) in crystallin beta 3 (*CRYBB3*; MIM*123630) (Supplementary Figure 4), which is likely to explain the bilateral cataracts observed in him (MIM#609741).[34] Variants that passed population and pathogenicity prediction filters but were not investigated further are detailed in Supplementary Table 3 for each family.

Patient (sex/age range)	Zygoty and variants (NM_012401.4, NP_036533.2)	Phenotype				
		Auditory	Dental	Developmental /neurological	Vision	Other
Family 1 II:3 (M/12-18)	Homozygous c.2413A>T: p.(Ile805Phe); c.2413A>T: p.(Ile805Phe)	SNHL	AI, conical permanent incisors	Global developmental delay, moderate intellectual disability	Myopia, horizontal nystagmus, (congenital cataract due to <i>CRYBB3</i> variant)	Ear lobe skin blind-ended tracts
Family 1 II:6 (M/19-21)	Homozygous c.2413A>T: p.(Ile805Phe); c.2413A>T: p.(Ile805Phe)	SNHL; labyrinthine malformation	AI, conical permanent incisors	Global developmental delay, epilepsy, moderate intellectual disability	Severe myopia with scattered papillae, horizontal nystagmus, macular atrophy	Ear lobe skin blind-ended tracts, unilateral renal agenesis, pyloric stenosis, asthma, recurrent bronchitis, intrauterine growth retardation, finger pads, watch glass toe nails, overweight
Family 2 IV:2 (M/12-18)	Homozygous c.2248G>A: p.(Asp750Asn); c.2248G>A: p.(Asp750Asn)	SNHL	AI	Intellectual disability	No obvious abnormality, not examined	
Family 3 II:1 (M/6-11)	Compound heterozygous c.750C>A: p.(Cys250*); c.3117G>A: p.(Thr1039=)	SNHL (mild) 500-4000 Hz,	AI with hypoplasia	Normal	Developmental macular abnormality with pale fundus, attenuated blood vessels, high myopia, nystagmus, microcornea	Ear lobe skin blind-ended tracts, cleft palate, hypertelorism, keratopathy
Family 4 II:1 (F/19-21)	Compound heterozygous c.2606del: p.(Phe869Serfs*45); c.3982_3986del: p.(Phe1328His*65)	SNHL	AI; missing upper permanent lateral incisors	Normal	No obvious abnormality, not examined	Ear lobe skin blind-ended tracts, Bilateral primary lower limb lymphoedema (onset aged 3), nevus, cellulitis
Family 5 II:1 (F/50-59)	Homozygous c.5197- 337_5310del: p.(Asp1733_Arg1779del); c.5197-337_5310del: p.(Asp1733_Arg1779del) ..	SNHL	AI	Mild/moderate intellectual disability	No obvious abnormality, not examined	Bilateral primary lower limb lymphoedema

Patient (sex/age range)	Zygoty and variants (NM_012401.4, NP_036533.2)	Phenotype				
		Auditory	Dental	Developmental /neurological	Vision	Other
Family 5 II:2 (M/50-59)	Homozygous c.5197-337_5310del: p.(Asp1733_Met1770del) ; c.5197-337_5310del: p.(Asp1733_Met1770del)	SNHL	AI	Intellectual disability	No obvious abnormality, not examined	Unilateral lymphoedema of one foot
Family 6 III:1 (M/2-5)	Homozygous c.4609G>A: p.(Gly1537Ser); c.4609G>A: p.(Gly1537Ser)	Could not be assessed; no current indication of hearing loss	Clinical tooth failure (cause unclear); Could not be assessed further	Profound intellectual disability, non-verbal, autistic features, hyperactive behaviour	Strabismus, no other obvious abnormality, could not be assessed.	Mild generalised muscular hypotonia

Table 1. The variants in *PLXNB2* identified in six families and the disease features observed. Splicing prediction tools suggest that exon 35 is entirely skipped leading to p.(Asp1733_Arg1779del) instead of p.(Asp1733_Met1770del) as would be predicted from the proportion of the gene deleted. Age ranges are shown for individuals to maintain anonymity. Age of onset was from birth unless otherwise stated. Abbreviations used: AI amelogenesis imperfecta; SNHL sensorineural hearing loss. Variants are based on genome build GRCh37 and *PLXNB2* transcript ENST00000359337.9, NM_012401.4 and *PLXNB2* protein ENSP00000352288.4, NP_036533.2.

1
2
3
4 In Family 2, two Omani brothers born of a first cousin union, were found to have bilateral
5
6 SNHL, intellectual disability and AI (Table 1, Figure 1 and Supplementary Figure 5). Exome
7
8 sequencing of one affected brother revealed a homozygous missense variant in *PLXNB2*,
9
10 c.2248G>A, p.(Asp750Asn). This replaces a charged residue with an uncharged one,
11
12 affecting a highly conserved residue in the extracellular portion of the protein
13
14 (Supplementary Figure 3). SIFT predicts the variant to be deleterious and it was not identified
15
16 in gnomAD (Supplementary Table 2).
17
18

19
20 Family 3 was identified independently via the UK Inherited Retinal Dystrophy Consortium.
21
22 They are a white British family with an affected male child born with facial clefting, who
23
24 also presented with nystagmus shortly after birth. In middle childhood, he was diagnosed
25
26 with retinal dystrophy, high myopia, microcorneas and mild keratopathy. He also has mild
27
28 bilateral SNHL for sounds ranging from 500-4000 Hz, and AI (Table 1, Figures 1, 2 and
29
30 Supplementary Figure 6). Exome sequencing revealed biallelic compound heterozygous
31
32 variants in *PLXNB2*, one a nonsense variant, c.750C>A, p.(Cys250*), and one synonymous
33
34 variant altering the final base of the splice donor site of exon 19, predicted to affect splicing,
35
36 c.3117G>A, p.(Thr1039=). Analysis with splice prediction tools Splice AI[26] and
37
38 NetGene2[25] predicted loss of the donor site, suggesting that some of intron 19 may be
39
40 retained in the mature transcript (Supplementary Table 4, Supplementary Figure 7). Neither
41
42 variant was identified in gnomAD (Supplementary Table 2). A second fetus, who presented
43
44 with clefting, was electively aborted. Genotyping showed that the fetus was heterozygous for
45
46 the nonsense *PLXNB2* variant only.
47
48
49
50
51

52
53 Next, we searched the UK 100,000 Genomes dataset[35] for patients with biallelic variants in
54
55 *PLXNB2* and a similar phenotype. We identified one affected white British female (Family 4)
56
57 with SNHL, AI, lower limb lymphoedema and cellulitis (Table 1, Figures 1, 2,
58
59 Supplementary Figure 8). She carries biallelic compound heterozygous frameshift variants
60

1
2
3 c.2606delT, p.(Phe869Serfs*45) and c.3982_3986delCTTT, p.(Phe1328Hisfs*65) in
4
5 *PLXNB2* (Supplementary Figure 9), both predicted to produce transcripts that are subject to
6
7 nonsense mediated decay.[36] Variant c.2606delT, p.(Phe869Serfs*45) has previously been
8
9 identified in gnomAD as a heterozygous variant in one individual, suggesting an allele
10
11 frequency of 4.024×10^{-6} . Variant c.3982_3986delCTTT, p.(Phe1328Hisfs*65) was not
12
13 present in gnomAD.
14
15

16
17 With increased understanding of the clinical presentation associated with biallelic *PLXNB2*
18
19 variants, we identified Family 5 through further collaboration. Two affected siblings of
20
21 Pakistani origin, born of a consanguineous union (Figure 1) presented with deafness, AI,
22
23 intellectual disability and lower limb lymphoedema (Figure 2, Table 1, Supplementary
24
25 Figures 10, 11). Exome sequencing of II:1 and subsequent Exome Depth analysis revealed a
26
27 homozygous deletion spanning exons 34 and 35 (Reads ratio 0.0291, Bayes factor 18.3;
28
29 Supplementary Table 2). The breakpoints predicted in the exome sequence (Supplementary
30
31 Figure 12), chr22:50,715,085 and chr22:50,715,672, were confirmed by PCR, which also
32
33 confirmed the deletion was present in II:2. This deletion is in-frame and is predicted to delete
34
35 at least 38 amino acids (aa) (p.(Asp1733_Met1770del) from the 1838aa protein, including all
36
37 of exon 34 and part of exon 35. Splice prediction tool NetGene2 (v2.4.2) predicts that exon
38
39 35 will be skipped entirely (Supplementary Table 5), resulting in an in-frame deletion of
40
41 47aa, p.(Asp1733_Arg1779del), suggesting that an abnormal *PLXNB2* protein may be
42
43 produced. The deleted region is part of the Rho-GAP catalytic domain critical to the protein's
44
45 function, but the deletion would leave the catalytic arginine residues at 1395, 1396 and 1691
46
47 intact.
48
49
50
51
52
53

54
55 Using GeneMatcher,[37] we identified one further patient with biallelic *PLXNB2* variants and
56
57 an overlapping disease phenotype. Family 6 are of Iraqi origin. One affected male was born
58
59 of first cousin consanguineous parents (Figure 1). In early childhood, he has severe
60

1
2
3 developmental delay and autistic features, and his tooth enamel shows evidence of severe
4 damage from a limited visual inspection (Table 1, Supplementary Figure 13). However, it
5 was not possible to carry out a detailed dental examination or to obtain dental radiographs.
6
7

8
9
10 The presence of AI, as opposed to severe caries could therefore not be confirmed, and testing
11 for SNHL and eye disease was not possible. Upon exome sequencing, the affected individual
12 was found to carry a homozygous *PLXNB2* variant c.4609G>A, p.(Gly1537Ser), which
13 affects the highly conserved Rho-GAP domain that lies within the intracellular portion of
14
15
16
17
18
19
20
21
22
23
24
25
26
27
28
29
30
31
32
33
34
35
36
37
38
39
40
41
42
43
44
45
46
47
48
49
50
51
52
53
54
55
56
57
58
59
60
PLXNB2 and changes the residue from a non-polar to a polar residue (Table 1,
Supplementary Table 2, Supplementary Figure 3). The residue is conserved in all species
examined and this variant was not present in gnomAD.

We next used iTASSER MTD to try to assess the effect of each of the variants on the overall
predicted structure of PLXNB2 (Supplementary Figure 14). *In silico* predictions of WT
PLXNB2 structure (panel A) and of these variants are likely to be of limited use due the
small percentage of PLXNB2 covered by known crystal structures and the lack of appropriate
homologous protein structures upon which to base the WT structure. The local structural
changes for the missense variants (Asp750Asn, Ile805Phe and Gly1537Ser) are shown in
panels B, C and D. There were minor changes in the solvent accessibility for Asp750Asn and
Ile805Phe. For Ile805Phe, the mutant structure is characterized as undefined, in comparison
to the WT strand structure. The model for the deletion Asp1733_Arg1779del shows extensive
structural differences to the WT protein.

To gain insight into *Plxnb2* expression in mice, we performed *in situ* hybridization using a
digoxigenin-labeled antisense riboprobe generated from the same DNA template as
previously used by the EURExpress consortium (www.eurexpress.org) (Supplementary
Figure 15). Mouse embryos were analyzed at E14.5, E16.5 and E19.5. *Plxnb2* expression was
detected in the kidney and lung (Fig. 3A and B). Discrete expression was observed in the

1
2
3 developing inner ear (cochlea: Fig. 3C). Expression was also detected in olfactory epithelium
4
5 and retina (Fig. 3D and F), and in the small and large intestine (Fig. 3E).
6
7

8
9 We also interrogated the GTEx portal[38] (<https://gtexportal.org/>) to determine the
10
11 expression of *PLXNB2* in human tissues. This showed that there was relatively high
12
13 expression of *PLXNB2* in the cerebellum and cerebellar hemisphere compared to other
14
15 regions of the brain. There was also high expression in the kidney, salivary gland, ovary,
16
17 prostate, spleen and thyroid, amongst other tissues (Supplementary Figure 16).
18
19

20
21 Since all individuals studied had AI or were suspected to have AI, we investigated the
22
23 expression of *Plxnb2* in the mouse during various stages of tooth development (Fig. 3G, I and
24
25 K lower molar and H, J and L lower incisor). *Plxnb2* transcripts were observed at E14.5 in
26
27 the epithelial tissues of the developing teeth, at E16.5 in the epithelial and mesenchymal
28
29 compartments of the incisor and in the epithelial part of the molar. At E19.5 labeling was
30
31 observed in differentiating ameloblasts.
32
33
34
35
36
37
38
39
40
41
42
43
44
45
46
47
48
49
50
51
52
53
54
55
56
57
58
59
60

Discussion

Here we describe biallelic pathogenic variants in *PLXNB2* in six families of diverse ethnicity with individuals affected by a variable syndromic phenotype. Four of these are consanguineous families with affected individuals homozygous for an extremely rare variant that has almost certainly been passed down both branches of the family, and one includes affected cousins, demonstrating significant co-segregation of the disease with biallelic *PLXNB2* variants. This syndrome has AI and SNHL as core symptoms, and intellectual disability, lower limb lymphoedema, ocular abnormalities and a variety of other conditions are also seen in some, but not all, cases. Given the varied and complex roles of *PLXNB2* in development,[1] it seems unsurprising that biallelic variants cause a syndromic disease phenotype. The variants all have pathogenicity scores indicating that they are predicted to be deleterious (Supplementary Table 2). The case series we have accumulated, together with published evidence of an overlapping condition in *Plxnb2* knockout mice, provides compelling evidence for biallelic variants in *PLXNB2* as the cause of this recessively inherited condition.

All variants implicated are extremely rare, with all but one absent in gnomAD (v2.1.1), which contains approximately 124,000 individuals with good quality sequence across *PLXNB2*. The rarity of these variants, together with the constraint metrics available in gnomAD (o/e = 0.19, pLI = 0.99),[39] suggest that *PLXNB2* loss-of-function variants are not well tolerated and affect viability. However, the identification of an individual who may entirely lack *PLXNB2* (Family 4 II:1) seems to contradict this. This is consistent with observations in *Plxnb2* knockout mice, where homozygosity for the knockout allele was lethal on one genetic background but viable on another.[12, 13] The *PLXNB2* variants identified herein include missense, frameshift and splice variants, a premature termination

1
2
3 codon and a deletion spanning two exons, which are all observed to be protein damaging
4
5 variants.
6
7
8
9

10 One possible interpretation of these findings is that all the observed human variants have the
11 effect of being functional knockouts, and that, as observed in mouse models, the viability of
12 such embryos is determined by the genetic background. Genetic background might also
13 explain the highly variable phenotypes observed in different cases, with only AI and SNHL
14 as consistent features. Pathogenic variants in *PLXNA1* cause an overlapping and similarly
15 varying range of phenotypes to pathogenic variants in *PLXNB2*. [23]. The impact of genetic
16 background on variation in disease phenotype, severity and survival, has been noted for one
17 *Plxnb2*^{-/-} mouse model, [12] which suggests that other cosegregating variants may affect
18 disease range and severity. This may suggest that, in spite of the distinct patterns of plexin
19 expression, [8] other plexins can sometimes partially compensate for loss of PLXNB2 or
20 PLXNA1 to allow developmental processes vital to life to proceed. However, to prove such
21 an effect would require the study of a large cohort of cases, and as yet no specific variants
22 have been implicated in phenotype variation in either of these syndromes. Given that this
23 cohort consists of only eight individuals with six different biallelic genotypes, the power to
24 detect any genotype-phenotype correlation in this study is very limited.
25
26
27
28
29
30
31
32
33
34
35
36
37
38
39
40
41
42
43
44
45
46

47 Alternatively, the *PLXNB2* variants and/or genotypes in the families described herein may
48 each have unique effects on PLXNB2 function. Variants could cause partial loss-of-function
49 through hypomorphic alleles, with expression of the normal transcript reduced but not
50 abolished, [40], or may act as “gain-of-function” alleles, creating a protein with altered or
51 enhanced function or inappropriate persistence within the cell. Consistent with this
52
53
54
55
56
57
58
59
60

1
2
3 hypothesis, the affected cousins in family 1 and affected siblings in family 5, each having the
4 same genotype, have remarkably similar phenotypes (Table 1).
5
6
7
8
9

10 The missense variants identified in this study affect both the extracellular (p.(Ile805Phe) and
11 p.(Asp750Asn)) and intracellular portions of the protein (p.(Gly1537Ser)), with no particular
12 region or domain specifically affected by the variants identified in this study. In order to
13 assess the effects of the variants on protein structure, we attempted to model the changes
14 using I-TASSER-MTD.[32] However, due to the lack of homologous structures available for
15 the majority of the *PLXNB2* protein, including the regions affected by the variants, the
16 accuracy of the modelling is likely to be low. The variants identified herein could be altering
17 the binding of *PLXNB2* to semaphorins via the sema domain, the subsequent
18 homodimerization of *PLXNB2* upon binding semaphorin, catalytic activity via the GAP
19 domain and interaction with GTPases, or the ability to interact with other proteins and to
20 effect other types of downstream signalling.[41] Further investigation will be required to
21 better understand the effects of specific variants and the basis of variation on phenotype in
22 the condition caused by *PLXNB2* variants.
23
24
25
26
27
28
29
30
31
32
33
34
35
36
37
38
39
40
41

42 Heterozygous carriers of the variants identified in these families appear in general to be
43 unaffected by disease, although one fetus (Family 3 II:2) did have facial clefting and carried a
44 heterozygous nonsense *PLXNB2* variant (c.750C>A, p.(Cys250*)). It is unknown whether
45 this fetus would have developed other clinical features similar to their sibling. It is possible
46 that another variant could be partially or entirely responsible for this particular phenotype
47 rather than the *PLXNB2* variant. In individuals with *PLXNA1* pathogenic variants, disease has
48 been observed with both biallelic and particular de novo heterozygous variants.[23]
49
50
51
52
53
54
55
56
57
58
59
60

1
2
3 The core phenotypes observed for the individuals carrying pathogenic *PLXNB2* variants
4 reflect negative impacts on the development or function of the cochlea and ameloblasts. This
5
6 led us to consider whether other plexins are expressed in the cochlea and inner enamel
7
8 epithelium at a similar time to *PLXNB2*, or whether *PLXNB2* is expressed alone in these
9
10 tissues, excluding the possibility of partial compensation by a closely related protein. Our
11
12 investigation of the expression of *Plxnb2* transcripts within the dental tissues of murine
13
14 embryos gave similar results to the expression patterns previously detailed by Perala et al.[8]
15
16 Their analysis of the expression of plexins in murine embryos using in situ hybridization
17
18 revealed that *Plxnb2* transcripts are present in the brain, retina, cochlea and tooth bud at
19
20 E14.[8] *Plxnb2* is the only plexin to be expressed at this time-point in all four tissues,
21
22 although the expression of *Plxnd1* was not examined in this study and the expression of other
23
24 plexins, most notably *Plxnb1*, do overlap that of *Plxnb2* in many tissues. *Plxnb2*, *Plxna2* and
25
26 *Plxna3* transcripts are all expressed in the cochlea, although the relative levels of expression
27
28 of each were not determined. Similarly, *Plxnb1* and *Plxnb2* transcripts were detected at
29
30 relatively high levels at E14 in the oral epithelium and tooth bud, but other plexins were also
31
32 detected at lower levels of expression. *Plxnb2* was shown to be expressed at relatively high
33
34 levels in the inner enamel epithelium at E15, with expression sustained until at least E16.
35
36 These findings suggest that *PLXNA2*, *PLXNA3* and *PLXNB1* are co-expressed in affected
37
38 tissues at relevant timepoints, but are unlikely to be able to fully compensate for the loss of
39
40 *PLXNB2*.

41
42 The variable phenotype and extremely low population frequency of the variants reported in
43
44 this study may be the reasons why pathogenic variants in *PLXNB2* have not previously been
45
46 reported as causing syndromic disease in humans. We suggest that the tooth enamel
47
48 phenotype, AI, is a consistent, but potentially easily missed feature that flags this genetic
49
50 diagnosis. AI is a heterogeneous group of genetic conditions characterized by a deficit in
51
52
53
54
55
56
57
58
59
60

1
2
3 enamel quantity and/or quality affecting all teeth of both dentitions.[42-44] It can present as
4
5 an isolated disease or can be part of more complex and diverse syndromes affecting other
6
7 tissues and organs. Once formed and following tooth eruption, enamel has no capacity for
8
9 cellular repair. Accordingly, AI provides a clear and persistent marker of abnormal
10
11 development that is recognisable at an early age. However, due to the presence of neuronal
12
13 deficits such as hearing loss and intellectual disability, AI might easily be overlooked or
14
15 dismissed as dental caries due to suboptimal diet and/or poor dental hygiene. A differential
16
17 diagnosis of AI as opposed to fluorosis or molar incisor hypomineralisation is also a possible
18
19 confounding issue. Diagnosis of AI may therefore require a specialist paediatric dental
20
21 professional. The disconnection between dental and general healthcare also presents barriers
22
23 to diagnosis and has been flagged as problematic previously in the differential diagnosis of
24
25 Usher and Heimler syndromes.[45]
26
27
28
29

30
31
32 The families presented have AI characterised by variable abnormalities of enamel volume
33
34 (hypoplasia) and mineralisation (hypomineralised). This is consistent with the understanding
35
36 of *PLXNB2* function. Future laboratory investigation of enamel from affected individuals
37
38 will give insight into the characteristics of the disruption to enamel rod morphology and
39
40 mineralisation. It is unclear if the other dental morphological changes reported, including
41
42 conical lateral incisors, missing lateral incisors, flattened occlusal surfaces and mild
43
44 taurodontism are consequent to *PLXNB2* functional disruption or are coincidence in these
45
46 families. As further families are described, the core features of the dental phenotype will
47
48 become clearer and will be an important clinical indicator to consider *PLXNB2* further.
49
50
51

52
53
54 In conclusion, we identify biallelic pathogenic variants in *PLXNB2* as a cause of a new
55
56 autosomal recessively inherited, phenotypically diverse syndrome including AI and SNHL as
57
58
59
60

1
2
3 core symptoms, with intellectual disability, ocular disease, ear developmental abnormalities
4
5 and lymphoedema also present in multiple cases.
6
7

8 9 **Data Availability**

10
11
12 Raw sequencing data supporting the findings of this study are available from the
13
14 corresponding author upon request.
15
16

17 18 **Acknowledgements**

19
20 We would like to thank all of the families involved in this study, as well as the patient
21
22 support group Amélogénèse France <https://amelogeneseFrance.wixsite.com/amelogenese>. We
23
24 thank C. Stoetzel and M. Prasad, University of Strasbourg, J. Clayton-Smith, University of
25
26 Manchester and S. Al-Bahlani, Al Nadha Hospital, Muscat, Oman, for their help in the first
27
28 steps of this project.
29
30

31
32 The Genotype-Tissue Expression (GTEx) Project was supported by the Common Fund of the
33
34 Office of the Director of the National Institutes of Health, and by NCI, NHGRI, NHLBI,
35
36 NIDA, NIMH, and NINDS. The data used for the analyses described in this manuscript were
37
38 obtained from: <https://gtexportal.org/home/gene/PLXNB2> on the GTEx portal on 21st July
39
40
41 2023.
42
43

44 45 **Competing Interests**

46
47
48 The authors declare no competing interests.
49
50

51 52 **Funding**

53
54 This work was supported by Rosetrees Trust Grant PGS19-2/10111, Retina UK and Fight for
55
56 Sight UK (RP Genome Project GR586), the Wellcome Trust [grant number 093113], the
57
58 French Ministry of Health (National Program for Clinical Research, PHRC 2008 N°4266
59
60

1
2
3 Amelogenesis imperfecta), the University Hospital of Strasbourg (HUS, API, 2009–2012,
4 ‘Development of the oral cavity: from gene to clinical phenotype in Human’) and the grant
5 ANR-10-LABX-0030-INRT, a French State fund managed by the Agence Nationale de la
6 Recherche under the frame programme Investissements d’Avenir labelled ANR-10-IDEX-
7 0002-02. It was also financed by and contributed to the actions of the project No. 1.7
8 “RARENET: a tri-national network for education, research and management of complex and
9 rare disorders in the Upper Rhine” co-financed by the European Regional Development Fund
10 (ERDF) of the European Union in the framework of the INTERREG V and previously
11 INTERREG IV Upper Rhine program as well as to the ERN (European reference network)
12 CRANIO initiative. ABZ is a USIAS 2015 Fellow of the Institute of Advanced Studies
13 (Institut d’Etudes Avancées) de l’Université de Strasbourg, France. UH is the recipient of a
14 Leeds Doctoral Scholarship (LDS). This work is part of the Projet E-GENODENT financed
15 by the Fonds d’Intervention Régionale (FIR) of the Agence Régionale de Santé Grand Est
16 (2019-2022). We are grateful for funding provided by Filière TETECOUC and “Pierre Henri et
17 ses amis” patient support groups.

37 Collaborator Statement

38 The UK Inherited Retinal Dystrophy Consortium (UKIRDC) includes, in addition to listed
39 authors CELS, RLT, GCB, and CFI, Martin McKibbin, Manir Ali, Carmel Toomes, Stuart
40 Ingram, Forbes Manson, Panagiotis Sergouniotis, Gavin Arno, Alison J Hardcastle, Andrew
41 Webster, Nikolas Pontikos, Michael Cheetham, Alessia Fiorentino, Susan Downes, Jing Yu,
42 Stephanie Halford, Suzanne Broadgate and Veronica van Heyningen.

43 The Genomes England Research Consortium (GERC) includes Ambrose JC¹, Arumugam P¹,
44 Bevers R¹, Bleda M¹, Boardman-Pretty F^{1,2}, Boustred CR¹, Brittain H¹, Brown MA¹,
45 Caulfield MJ^{1,2}, Chan GC¹, Giess A¹, Griffin JN¹, Hamblin A¹, Henderson S^{1,2}, Hubbard

1
2
3 TJP¹, Jackson R¹, Jones LJ^{1,2}, Kasperaviciute D^{1,2}, Kayikci M¹, Kousathanas A¹, Lahnstein
4 L¹, Lakey A¹, Leigh SEA¹, Leong IUS¹, Lopez FJ¹, Maleady-Crowe F¹, McEntagart M¹,
5
6 Minneci F¹, Mitchell J¹, Moutsianas L^{1,2}, Mueller M^{1,2}, Murugaesu N¹, Need AC^{1,2},
7
8 O'Donovan P¹, Odhams CA¹, Patch C^{1,2}, Perez-Gil D¹, Pereira MB¹, Pullinger J¹, Rahim T¹,
9
10 Rendon A¹, Rogers T¹, Savage K¹, Sawant K¹, Scott RH¹, Siddiq A¹, Sieghart A¹, Smith SC¹,
11
12 Sosinsky A^{1,2}, Stuckey A¹, Tanguy M¹, Taylor Tavares AL¹, Thomas ERA^{1,2}, Thompson
13
14 SR¹, Tucci A^{1,2}, Welland MJ¹, Williams E¹, Witkowska K^{1,2}, Wood SM^{1,2}, Zarowiecki M¹
15
16
17
18
19 1. Genomics England, London, UK

20
21
22 2. William Harvey Research Institute, Queen Mary University of London, London. EC1M
23
24 6BQ, UK.

25 26 27 **Contributorship Statement**

28
29 Conceptualization: CFI, AJM, ABZ; Data Curation: CELS, VL, UKIRDC, GERC, RGF, GN,
30
31 AR; Formal Analysis: CELS, VL, UH, SB, RLT, RGF, JAM, CMW; Funding Acquisition:
32
33 CFI, AJM, ABZ; Investigation: CELS, VL, UH, SB, RLT, JCS, JP, UKIRDC, GERC, SBW,
34
35 RGF, JAM, SA-B, GCB, SM, AJM, ABZ; Methodology: CELS, VL, UH, SB, RLT, JAP,
36
37 UKIRDC, GERC, SBW, RGF, JAM, CFI, AJM, ABZ; Project administration: CELS, CFI,
38
39 AJM, ABZ; Resources: GERC; Supervision: CELS, JAP, CMW, CFI, AJM; Validation:
40
41 CELS, VL, UH, RLT, RGF; Visualization: CELS, VL, UH, SB, GN, AR, SBW, RGF, SM,
42
43 AJM, ABZ; Writing-original draft: CELS, VL; Writing-review & editing: CELS, CMW, CFI,
44
45 AJM, ABZ. All authors reviewed and commented critically on the final draft.
46
47
48
49
50
51

52 53 **Ethics Declaration**

54
55 This study underwent ethical review by the National Research Ethics Service Committee for
56
57 Yorkshire & the Humber – South Yorkshire REC ref 13/YH/0028 IRAS project ID 82448
58
59
60

1
2
3 and underwent local ethical approval at other centers involved in this study. The 100,000
4
5 Genomes Project is covered by REC reference approval 14/EE/1112.
6
7
8
9

10 **References**

- 11
12 1 Perälä N, Sariola H and Immonen T. More than nervous: the emerging roles of plexins.
13
14 *Differentiation* 2012;83:77-91. doi:10.1016/j.diff.2011.08.001
15
16
17 2 Alto LT and Terman JR. Semaphorins and their Signaling Mechanisms. *Methods Mol Biol*
18
19 2017;1493:1-25. doi:10.1007/978-1-4939-6448-2_1
20
21
22 3 Maestrini E, Tamagnone L, Longati P, *et al.* A family of transmembrane proteins with
23
24 homology to the MET-hepatocyte growth factor receptor. *Proc Natl Acad Sci U S A*
25
26 1996;93:674-8. doi:10.1073/pnas.93.2.674
27
28
29 4 Tamagnone L, Artigiani S, Chen H, *et al.* Plexins are a large family of receptors for
30
31 transmembrane, secreted, and GPI-anchored semaphorins in vertebrates. *Cell* 1999;99:71-80.
32
33 doi:10.1016/s0092-8674(00)80063-x
34
35
36 5 Alves CH, Sanz AS, Park B, *et al.* Loss of CRB2 in the mouse retina mimics human
37
38 retinitis pigmentosa due to mutations in the CRB1 gene. *Hum Mol Genet* 2013;22:35-50.
39
40 doi:10.1093/hmg/dd3398
41
42
43 6 Swiercz JM, Kuner R, Behrens J, *et al.* Plexin-B1 directly interacts with PDZ-
44
45 RhoGEF/LARG to regulate RhoA and growth cone morphology. *Neuron* 2002;35:51-63.
46
47 doi:10.1016/s0896-6273(02)00750-x
48
49
50 7 Perrot V, Vazquez-Prado J and Gutkind JS. Plexin B regulates Rho through the guanine
51
52 nucleotide exchange factors leukemia-associated Rho GEF (LARG) and PDZ-RhoGEF. *J*
53
54 *Biol Chem* 2002;277:43115-20. doi:10.1074/jbc.M206005200
55
56
57 8 Perälä NM, Immonen T and Sariola H. The expression of plexins during mouse
58
59 embryogenesis. *Gene Expr Patterns* 2005;5:355-62. doi:10.1016/j.modgep.2004.10.001
60

- 1
2
3 9 Worzfeld T, Püschel AW, Offermanns S, *et al.* Plexin-B family members demonstrate non-
4
5 redundant expression patterns in the developing mouse nervous system: an anatomical basis
6
7 for morphogenetic effects of Sema4D during development. *Eur J Neurosci* 2004;19:2622-32.
8
9 doi:10.1111/j.0953-816X.2004.03401.x
10
11
12 10 Luukko K and Kettunen P. Integration of tooth morphogenesis and innervation by local
13
14 tissue interactions, signaling networks, and semaphorin 3A. *Cell Adh Migr* 2016;10:618-26.
15
16 doi:10.1080/19336918.2016.1216746
17
18
19 11 Zhang L, Han Y, Chen Q, *et al.* Sema4D-plexin-B1 signaling in recruiting dental stem
20
21 cells for vascular stabilization on a microfluidic platform. *Lab Chip* 2022;22:4632-44.
22
23 doi:10.1039/d2lc00632d
24
25
26 12 Friedel RH, Kerjan G, Rayburn H, *et al.* Plexin-B2 controls the development of cerebellar
27
28 granule cells. *J Neurosci* 2007;27:3921-32. doi:10.1523/jneurosci.4710-06.2007
29
30
31 13 Deng S, Hirschberg A, Worzfeld T, *et al.* Plexin-B2, but not Plexin-B1, critically
32
33 modulates neuronal migration and patterning of the developing nervous system in vivo. *J*
34
35 *Neurosci* 2007;27:6333-47. doi:10.1523/jneurosci.5381-06.2007
36
37
38 14 Zhao N, Ruan M, Koestler DC, *et al.* Epigenome-wide scan identifies differentially
39
40 methylated regions for lung cancer using pre-diagnostic peripheral blood. *Epigenetics*
41
42 2022;17:460-72. doi:10.1080/15592294.2021.1923615
43
44
45 15 Liu H and Zhao H. Prognosis related miRNAs, DNA methylation, and epigenetic
46
47 interactions in lung adenocarcinoma. *Neoplasia* 2019;66:487-93.
48
49 doi:10.4149/neo_2018_181029N805
50
51
52 16 Lin L, Wang Y, Bian S, *et al.* A circular RNA derived from PLXNB2 as a valuable
53
54 predictor of the prognosis of patients with acute myeloid leukaemia. *J Transl Med*
55
56 2021;19:123. doi:10.1186/s12967-021-02793-7
57
58
59
60

1
2
3 17 Saez-Atienzar S, Bandres-Ciga S, Langston RG, *et al.* Genetic analysis of amyotrophic
4 lateral sclerosis identifies contributing pathways and cell types. *Sci Adv* 2021;7.
5
6

7
8 doi:10.1126/sciadv.abd9036
9

10 18 Huang Y, Tejero R, Lee VK, *et al.* Plexin-B2 facilitates glioblastoma infiltration by
11 modulating cell biomechanics. *Commun Biol* 2021;4:145. doi:10.1038/s42003-021-01667-4
12
13

14 19 Yin J, Chun CA, Zavadenko NN, *et al.* Next Generation Sequencing of 134 Children with
15 Autism Spectrum Disorder and Regression. *Genes* 2020;11:853. 10.3390/genes11080853.
16
17

18 20 Hemida AS, Mareae AH, Elbasiony ASA, *et al.* Plexin-B2 in psoriasis; a clinical and
19 immunohistochemical study. *J Immunoassay Immunochem* 2020;41:718-28.
20
21

22
23 doi:10.1080/15321819.2020.1741385
24

25 21 Wang X, Shi W, Zhao S, *et al.* Whole exome sequencing in unexplained recurrent
26 miscarriage families identified novel pathogenic genetic causes of euploid miscarriage. *Hum*
27
28
29
30
31
32 *Reprod* 2023;38:1003-18. doi:10.1093/humrep/dead039

33 22 Guimier A, de Pontual L, Braddock SR, *et al.* Biallelic alterations in PLXND1 cause
34 common arterial trunk and other cardiac malformations in humans. *Hum Mol Genet*
35
36
37
38 2023;32:353-6. doi:10.1093/hmg/ddac084
39

40 23 Dworschak GC, Punetha J, Kalanithy JC, *et al.* Biallelic and monoallelic variants in
41 PLXNA1 are implicated in a novel neurodevelopmental disorder with variable cerebral and
42
43
44
45
46 eye anomalies. *Genet Med* 2021;23:1715-25. doi:10.1038/s41436-021-01196-9

47 24 Karczewski KJ, Francioli LC, Tiao G, *et al.* The mutational constraint spectrum quantified
48 from variation in 141,456 humans. *Nature* 2020;581:434-43. doi:10.1038/s41586-020-2308-7
49
50

51 25 Hebsgaard SM, Korning PG, Tolstrup N, *et al.* Splice site prediction in Arabidopsis
52 thaliana pre-mRNA by combining local and global sequence information. *Nucleic Acids Res*
53
54
55
56 1996;24:3439-52. doi:10.1093/nar/24.17.3439
57
58
59
60

- 1
2
3 26 Jaganathan K, Kyriazopoulou Panagiotopoulou S, McRae JF, *et al.* Predicting Splicing
4 from Primary Sequence with Deep Learning. *Cell* 2019;176:535-48.e24.
5
6
7 doi:10.1016/j.cell.2018.12.015
8
9
10 27 Rentzsch P, Schubach M, Shendure J, *et al.* CADD-Splice-improving genome-wide
11 variant effect prediction using deep learning-derived splice scores. *Genome Med* 2021;13:31.
12
13
14 doi:10.1186/s13073-021-00835-9
15
16
17 28 Ioannidis NM, Rothstein JH, Pejaver V, *et al.* REVEL: An Ensemble Method for
18 Predicting the Pathogenicity of Rare Missense Variants. *Am J Hum Genet* 2016;99:877-85.
19
20
21 doi:10.1016/j.ajhg.2016.08.016
22
23
24 29 Adzhubei IA, Schmidt S, Peshkin L, *et al.* A method and server for predicting damaging
25 missense mutations. *Nat Methods* 2010;7:248-9. doi:10.1038/nmeth0410-248
26
27
28 30 Kumar P, Henikoff S and Ng PC. Predicting the effects of coding non-synonymous
29 variants on protein function using the SIFT algorithm. *Nat Protoc* 2009;4:1073-81.
30
31
32 doi:10.1038/nprot.2009.86
33
34
35 31 Plagnol V, Curtis J, Epstein M, *et al.* A robust model for read count data in exome
36 sequencing experiments and implications for copy number variant calling. *Bioinformatics*
37
38
39 2012;28:2747-54. doi:10.1093/bioinformatics/bts526
40
41
42 32 Zhou X, Zheng W, Li Y, *et al.* I-TASSER-MTD: a deep-learning-based platform for
43 multi-domain protein structure and function prediction. *Nat Protoc* 2022;17:2326-53.
44
45
46 doi:10.1038/s41596-022-00728-0
47
48
49 33 Pettersen EF, Goddard TD, Huang CC, *et al.* UCSF Chimera--a visualization system for
50 exploratory research and analysis. *J Comput Chem* 2004;25:1605-12. doi:10.1002/jcc.20084
51
52
53 34 Reis LM, Tyler RC, Muheisen S, *et al.* Whole exome sequencing in dominant cataract
54 identifies a new causative factor, CRYBA2, and a variety of novel alleles in known genes.
55
56
57 *Hum Genet* 2013;132:761-70. doi:10.1007/s00439-013-1289-0
58
59
60

- 1
2
3 35 Smedley D, Smith KR, Martin A, *et al.* 100,000 Genomes Pilot on Rare-Disease
4
5 Diagnosis in Health Care - Preliminary Report. *N Engl J Med* 2021;385:1868-80.
6
7 doi:10.1056/NEJMoa2035790
8
9
10 36 Chang YF, Imam JS and Wilkinson MF. The nonsense-mediated decay RNA surveillance
11
12 pathway. *Annu Rev Biochem* 2007;76:51-74.
13
14 doi:10.1146/annurev.biochem.76.050106.093909
15
16
17 37 Sobreira N, Schiettecatte F, Valle D, *et al.* GeneMatcher: a matching tool for connecting
18
19 investigators with an interest in the same gene. *Hum Mutat* 2015;36:928-30.
20
21 doi:10.1002/humu.22844
22
23
24 38 Melé M, Ferreira PG, Reverter F, *et al.* Human genomics. The human transcriptome
25
26 across tissues and individuals. *Science* 2015;348:660-5. doi:10.1126/science.aaa0355
27
28
29 39 Lek M, Karczewski KJ, Minikel EV, *et al.* Analysis of protein-coding genetic variation in
30
31 60,706 humans. *Nature* 2016;536:285-91. doi:10.1038/nature19057
32
33
34 40 Bauwens M, Garanto A, Sangermano R, *et al.* ABCA4-associated disease as a model for
35
36 missing heritability in autosomal recessive disorders: novel noncoding splice, cis-regulatory,
37
38 structural, and recurrent hypomorphic variants. *Genet Med* 2019;21:1761-71.
39
40 doi:10.1038/s41436-018-0420-y
41
42
43 41 Pascoe HG, Wang Y and Zhang X. Structural mechanisms of plexin signaling. *Prog*
44
45 *Biophys Mol Biol* 2015;118:161-8. doi:10.1016/j.pbiomolbio.2015.03.006
46
47
48 42 Morr T. Amelogenesis imperfecta: More than just an enamel problem. *J Esthet Restor*
49
50 *Dent* 2023;35:745-57. doi:10.1111/jerd.13063
51
52
53 43 Dong J, Ruan W and Duan X. Molecular-based phenotype variations in amelogenesis
54
55 imperfecta. *Oral Dis* 2023, in press. doi:10.1111/odi.14599
56
57
58 44 Smith CEL, Poulter JA, Antanaviciute A, *et al.* Amelogenesis Imperfecta; Genes,
59
60 Proteins, and Pathways. *Front Physiol* 2017;8:435. doi:10.3389/fphys.2017.00435

1
2
3
4
5
6
7
8
9
10
11
12
13
14
15
16
17
18
19
20
21
22
23
24
25
26
27
28
29
30
31
32
33
34
35
36
37
38
39
40
41
42
43
44
45
46
47
48
49
50
51
52
53
54
55
56
57
58
59
60

45 Smith CE, Poulter JA, Levin AV, *et al.* Spectrum of PEX1 and PEX6 variants in Heimler syndrome. *Eur J Hum Genet* 2016;24:1565-71. doi:10.1038/ejhg.2016.62

Confidential: For Review Only

Figure legends

Figure 1. Pedigrees, Sanger sequencing and schematic diagram of the *PLXNB2* protein. **A.** DNA was available for all labelled individuals on each pedigree. Arrows indicate the individuals whose DNA was exome or genome sequenced. Affected status is as reported by the families for individuals for which DNA was not available. Sanger sequencing traces showing the segregation of each variant with disease in each family, except for family 5, for which this is shown in Supplementary Figure 9. The schematic diagram shows **B.** the *PLXNB2* transcript (ENST00000359337.9, NM_012401.4; 6409 bp) and **C.** the *PLXNB2* protein (ENSP00000352288.4, NP_036533.2; 1838 amino acids), with the positions marked for the pathogenic variants identified in this study.

Figure 2.

Clinical images that are illustrative of the shared and variable clinical features for affected individuals. **A.** The anterior clinical photograph showing primary teeth, the posterior teeth have changes consistent with loss of enamel (arrowheads) due to fracturing, whereas the enamel of the anterior teeth is developmentally thin and optically abnormal (Family 3 II:1). **B.** Panoramic radiograph of the adult permanent dentition illustrates that the enamel is more radiodense than the supporting dentine, but with a variably reduced enamel volume and irregular occlusal cusp morphology (arrowhead) consistent with AI characterised by enamel that is hypomineralised with variable hypoplasia (Family 4 II:2). **C.** SNHL was typical, with provision of hearing aids in childhood (Family 4 II:2). Blind-end skin tracts involving the skin of the ears or adjacent tissues (arrowhead) were observed in at least 3/6 families. **D.** Lower limb lymphoedema was observed in two families (Families 4 and 5, with Family 4 illustrated). **E.** Fundus autofluorescence images (Family 3 II:1) illustrate a developmental

1
2
3 macular abnormality with pale fundus and attenuated blood vessels. The individual also has
4
5 high myopia, nystagmus and microcornea.
6

7
8 **Figure 3.** Analysis of mouse *Plxnb2* transcript distribution by *in situ* hybridization. Selected
9
10 sections illustrating *Plxnb2* expression features in the developing skull bone, sensorial organs
11
12 and viscera are shown in the left-side panels (A–F), whereas right-side panels focus on
13
14 incisor (G, I and K) and molar (H, J and L) tooth development. Developmental stages and
15
16 section planes are: E14.5 frontal (A, B, G and H), E16.5 sagittal (C, D, E, I and J); E19.5
17
18 sagittal (F, K and L) sections. Am, ameloblasts; Co, cochlea; DP, dental papilla; EL,
19
20 epithelial loop; Gu, gubernaculum; IDE, inner dental epithelium; In, intestine; Ki, Kidney;
21
22 LI, lower incisor; Lu, lung; Od, odontoblasts; ODE, outer dental epithelium; OE, Olfactory
23
24 epithelium; Re, Retina; SB, skull bone; SR, stellate reticulum. Scale bars: 25 μm (J); 40 μm
25
26 (H and I); 50 μm (C and K); 60 μm (F and H), 80 μm (A D, E and L); 150 μm (B and G).
27
28
29
30
31
32
33
34
35
36
37
38
39
40
41
42
43
44
45
46
47
48
49
50
51
52
53
54
55
56
57
58
59
60

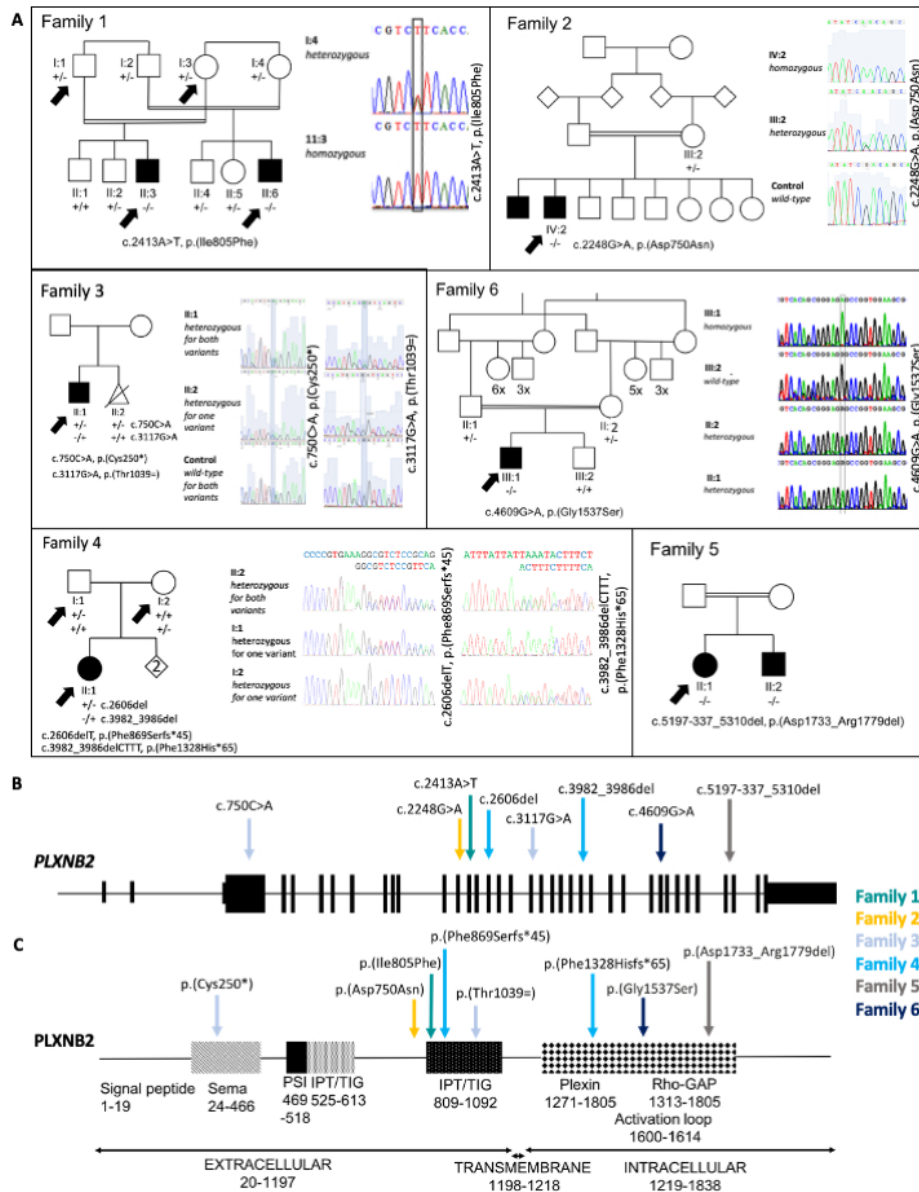


Figure 1. Pedigrees, Sanger sequencing and schematic diagram of the PLXNB2 protein. A. DNA was available for all labelled individuals on each pedigree. Arrows indicate the individuals whose DNA was exome or genome sequenced. Affected status is as reported by the families for individuals for which DNA was not available. Sanger sequencing traces showing the segregation of each variant with disease in each family, except for family 5, for which this is shown in Supplementary Figure 9. The schematic diagram shows B. the *PLXNB2* transcript (ENST00000359337.9, NM_012401.4; 6409 bp) and C. the PLXNB2 protein (ENSP00000352288.4, NP_036533.2; 1838 amino acids), with the positions marked for the pathogenic variants identified in this study.

190x245mm (96 x 96 DPI)

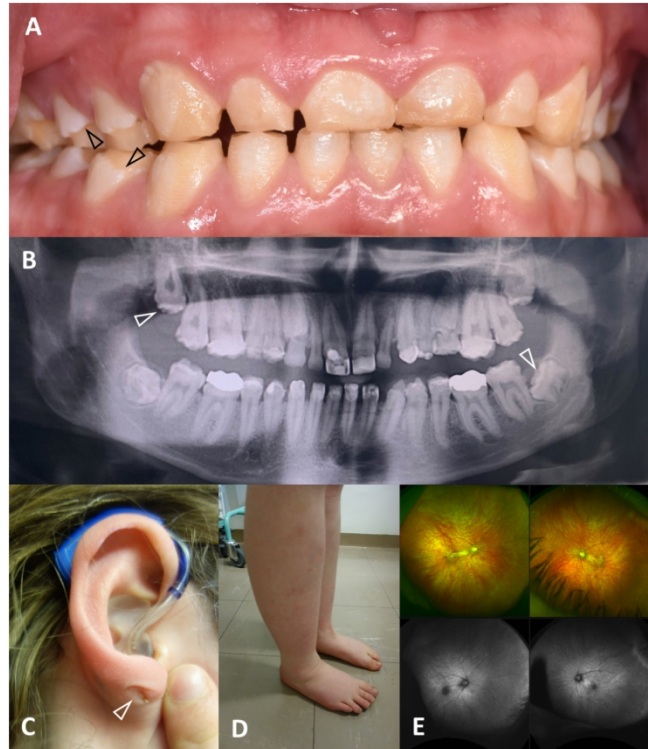


Figure 2. Clinical images that are illustrative of the shared and variable clinical features for affected individuals. A. The anterior clinical photograph showing primary teeth, the posterior teeth have changes consistent with loss of enamel (arrowheads) due to fracturing, whereas the enamel of the anterior teeth is developmentally thin and optically abnormal (Family 3 II:1). B. Panoramic radiograph of the adult permanent dentition illustrates that the enamel is more radiodense than the supporting dentine, but with a variably reduced enamel volume and irregular occlusal cusp morphology (arrowhead) consistent with AI characterised by enamel that is hypomineralised with variable hypoplasia (Family 4 II:2). C. SNHL was typical, with provision of hearing aids in childhood (Family 4 II:2). Blind-end skin tracts involving the skin of the ears or adjacent tissues (arrowhead) were observed in at least 3/6 families. D. Lower limb lymphoedema was observed in two families (Families 4 and 5, with Family 4 illustrated). E. Fundus autofluorescence images (Family 3 II:1) illustrate a developmental macular abnormality with pale fundus and attenuated blood vessels. The individual also has high myopia, nystagmus and microcornea.

190x245mm (233 x 233 DPI)

1
2
3
4
5
6
7
8
9
10
11
12
13
14
15
16
17
18
19
20
21
22
23
24
25
26
27
28
29
30
31
32
33
34
35
36
37
38
39
40
41
42
43
44
45
46
47
48
49
50
51
52
53
54
55
56
57
58
59
60

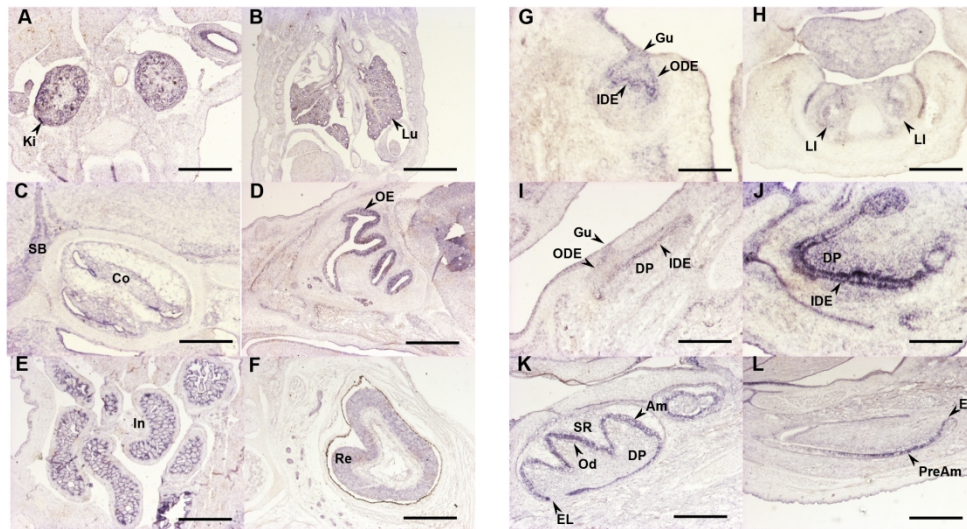


Figure 3. Analysis of mouse *Plxnb2* transcript distribution by in situ hybridization. Selected sections illustrating *Plxnb2* expression features in the developing skull bone, sensorial organs and viscera are shown in the left-side panels (A–F), whereas right-side panels focus on incisor (G, I and K) and molar (H, J and L) tooth development. Developmental stages and section planes are: E14.5 frontal (A, B, G and H), E16.5 sagittal (C, D, E, I and J); E19.5 sagittal (F, K and L) sections. Am, ameloblasts; Co, cochlea; DP, dental papilla; EL, epithelial loop; Gu, gubernaculum; IDE, inner dental epithelium; In, intestine; Ki, Kidney; LI, lower incisor; Lu, lung; Od, odontoblasts; ODE, outer dental epithelium; OE, Olfactory epithelium; Re, Retina; SB, skull bone; SR, stellate reticulum. Scale bars: 25 μm (J); 40 μm (H and I); 50 μm (C and K); 60 μm (F and H), 80 μm (A, D, E and L); 150 μm (B and G).

431x260mm (150 x 150 DPI)

Biallelic variants in Plexin B2 (*PLXNB2*) cause amelogenesis imperfecta, hearing loss and intellectual disability.

Claire E L Smith^{1*}, Virginie Laugel-Haushalter^{2*}, Ummey Hany¹, Sunayna Best^{1,3}, Rachel L Taylor^{4,5,6}, James A. Poulter¹, The UK Inherited Retinal Disease Consortium, Genomics England Research Consortium, Saskia B Wortmann^{7,8}, René G Feichtinger⁷, Johannes A Mayr⁷, Suhaila Al Bahlani⁹, Georgios Nikolopoulos¹⁰, Alice Rigby^{1,11}, Graeme C Black^{4,5}, Christopher M. Watson^{1,12}, Sahar Mansour^{13,14}, Chris F Inglehearn¹, Alan J Mighell^{11*} and Agnès Bloch-Zupan^{2,15,16*}

¹Leeds Institute of Medical Research, St James's University Hospital, University of Leeds, Beckett Street, Leeds. LS9 7TF. UK.

²Institut de Génétique et de Biologie Moléculaire et Cellulaire (IGBMC), INSERM U1258, CNRS-UMR7104, Université de Strasbourg, Illkirch, France.

³Yorkshire Regional Genetics Service, Leeds Teaching Hospitals NHS Trust, Leeds. LS7 4SA. UK.

⁴Division of Evolution and Genomic Sciences, Manchester Academic Health Science Centre, Faculty of Biology, Medicine and Health, School of Biological Sciences, University of Manchester, Manchester, M13 9NT. UK.

⁵Manchester Centre for Genomic Medicine, St. Mary's Hospital, Manchester University NHS Foundation Trust, Manchester. M13 9WL. UK.

⁶EMQN CIC, Pencroft Way, Manchester Science Park, Manchester. M15 6SE. UK.

⁷University Children's Hospital, Salzburger Landeskliniken (SALK) and Paracelsus Medical University (PMU), Müllner Hauptstrasse 48, 5020 Salzburg, Austria.

⁸Amalia Children's Hospital, Radboud University Medical Center, Geert Grooteplein Zuid 10, 6525 GA Nijmegen, the Netherlands.

⁹Dental & O.M.F.S Clinic, Al Nahdha Hospital, Ministry of Health, Muscat. HGQJ+GV6. Oman.

¹⁰Institute for Fundamental Biomedical Research, BSRC Alexander Fleming, 16672 Vari, Attica, Greece.

¹¹School of Dentistry, University of Leeds. LS2 9JT. UK.

¹²North East and Yorkshire Genomic Laboratory Hub, Central Lab, St. James's University Hospital, Leeds. LS9 7TF. UK.

¹³Lymphovascular Research Unit, Molecular and Clinical Sciences Research Institute, University of London St George's, London. SW17 0QT. UK.

¹⁴SW Thames Regional Genetics Service, St George's University Hospitals NHS Foundation Trust, London. SW17 0QT. UK.

¹⁵Faculté de Chirurgie Dentaire, Université de Strasbourg, 8 Rue Sainte Elisabeth, F-67000 Strasbourg, France.

¹⁶Centre de référence des maladies rares orales et dentaires O-Rares, Filière Santé Maladies rares TETE COU, European Reference Network CRANIO, Pôle de Médecine et Chirurgie Bucco-dentaires, Hôpital Civil, Hôpitaux Universitaires de Strasbourg (HUS), 1 place l'hôpital, 67000 Strasbourg, France.

* These authors contributed equally to the study.

Correspondence to:

Dr Claire E L Smith email C.E.L.Smith@leeds.ac.uk

Telephone (+44) 113 343 8445

Supplementary Materials and Methods.

Sequencing and analysis

Since individuals were recruited and sequenced by different institutions, the sequencing and filtering methods used vary and are detailed below.

Family 1

Regions of homozygosity were identified using the GeneChip® Human Mapping 250K *Nsp* assay (Affymetrix). Results were analysed using Affymetrix software. WES was performed by IntegraGen (Evry, France; <https://integragen.com>). WES and bioinformatic analysis followed the protocol previously described.[1] Briefly exons were captured using the SureSelect Human All Exon V5 + UTR 75 Mb reagent (Agilent Technologies, USA) and sequenced using an Illumina HiSeq 2000 sequencer (Illumina, USA). The Burrows-Wheeler Aligner (v7.12) was used to align reads to the Human genome reference sequence GRCh37. Variant calling was carried out using the HaplotypeCaller module of Genome Analysis Toolkit (GATK, v.3.4.36). Copy number variants were called using CANOES.[2] The variants were filtered to exclude variants with an allele frequency of more than 1% in public variation databases-including the 1,000 Genomes,[3] the Genome Aggregation Database (gnomAD) (v.2.2.1).[4] Variants in the 5' or 3' UTR and variants with intronic locations and no prediction of local splice effect, as well as synonymous variants without prediction of local splice effect were also filtered. Splice effects were predicted using MaxEntScan,[5] NNSplice[6] and SpliceSiteFinder.[7] Genes with homozygous and compound heterozygous variants consistent with a recessive mode of inheritance were prioritised for investigation.

Family 2

Three micrograms of genomic DNA were processed according to the SureSelect XT Library Prep protocol (Agilent Technologies, USA). SureSelect Human All Exon V5 (Agilent Technologies) was used as the exome capture reagent. Sequencing was performed using a 100 bp paired-end protocol on an Illumina HiSeq 2500 sequencer (Illumina, USA). The resulting fastq files were aligned to the human reference genome (GRCh37) using Burrows-Wheeler Aligner (BWA, v.0.7.12).[8] The alignment was processed according to GATK best practice. Exome depth was used for CNV analysis according to the developers' guidelines.[9]

Variants were filtered to exclude all changes other than missense, frameshift or stop variants, exonic insertion/deletions or variants located at splice consensus sites. Synonymous variants within the splice consensus region and predicted to affect splicing were also retained. Variants present in the gnomAD (v2.2.1)[4] were excluded if present at a frequency of 1% or higher. Variants were also filtered based on the mode of inheritance. In families known to be consanguineous, homozygous variants were prioritised. Variant lists were also filtered to exclude population specific high frequency variants and platform artefacts by removing variants also present in exomes of individuals of the same ethnicity without dental disease sequenced using the same reagents and platform.

Family 3

One microgram of genomic DNA was processed according to the Agilent SureSelect XT Library Prep protocol (Agilent Technologies). SureSelect Human All Exon V6 (Agilent Technologies) was used as the exome capture reagent. Whole exome libraries were sequenced with a 150 bp paired-end protocol on an Illumina Hi-Seq 3000 sequencer. Alignment, variant calling and filtering were as previously described for Family 2.

Family 4

Investigation of the 100,000 genomes rare disease dataset[10] was carried out using the Gene-Variant Workflow script (available from <https://research-help.genomicsengland.co.uk/display/GERE/Gene-Variant+Workflow>). This identified all *PLXNB2* variants from all available genome VCF files and annotated them using Ensembl Variant Effect Predictor. A custom Python script called `filter_gene_variant_workflow.py` (available from https://github.com/sunaynabest/filter_100K_gene_variant_workflow) was used to exclude common variants using the following criteria: 100K major allele frequency (MAF) ≥ 0.002 ; gnomAD allele frequency (AF) ≥ 0.002 and variants called in non-canonical transcripts. Variants were prioritised if they were also marked deleterious by SIFT. Individuals with biallelic high impact variants (variants annotated by VEP as 'high impact' include `stop_gained`, `stop_lost`, `start_lost`, `splice_acceptor_variant`, `splice_donor_variant`, `frameshift_variant`, `transcript_ablation`, `transcript_amplification`) were prioritised for study. Variants were excluded if they were only identified in unaffected relatives and not identified in probands. Variant segregation was confirmed by examining the accompanying genome data from parents.

Family 5

50 ng of genomic DNA was processed according to the Human Comprehensive Exome kit (Twist Bioscience) protocol. The exome library was sequenced using an Illumina P3 300 cycle kit on an Illumina NextSeq2000 instrument.

After checking the quality of the raw data by FastQC software (<https://www.bioinformatics.babraham.ac.uk/projects/fastqc/>) and adaptor trimming by Trim Galore (https://www.bioinformatics.babraham.ac.uk/projects/trim_galore/), sequence alignments were generated against the reference genome (hg19/GRCh37) using the BWA (v0.7.12-r1.39).[8] SAMtools was used to convert SAM files to BAM files and PCR duplicates were removed by Picard (v2.5.0), to produce sorted BAM files.

Variants were filtered to exclude all changes other than missense, frameshift or stop variants, exonic small insertion/deletions or variants located at splice consensus sites. Synonymous variants within the splice consensus region and predicted to affect splicing were also retained. Identified variants were excluded if the CADD (v1.6) score was < 15 or minor allele frequency (MAF) was > 0.01 . The filtered variant list was examined for candidate pathogenic variants in known or potential candidate AI or sensorineural hearing loss genes.

The sorted BAM files were used for custom CNV detection using a pipeline based on the R package ExomeDepth (v1.1.12) using default parameters.[9] A custom reference panel was created using BAM files from another 47 samples sequenced in the same run. Common CNVs[11] were filtered out and CNVs calls prioritised by Bayes factor (the \log_{10} of the likelihood ratio of data for the CNV call divided by that of the normal copy number call).

Soft clipped reads were visualised in Integrated Genomics Viewer to identify CNV breakpoints.

Family 6

Whole exome libraries were prepared from genomic DNA using the SureSelect60Mbv6 (Agilent) reagent using a 100 bp paired-end protocol on a HiSeq 4000 platform (Illumina). Reads were aligned to GRCh37/hg19 using the BWA (v.0.5.87.5).[8] Detection of genetic variation was performed using PINDEL (v 0.2.4t),[12] and ExomeDepth (v 1.0.0).[9] The

1
2
3 cut-off for biallelic inheritance was set to <0.01 allele frequency. The size of reference entries
4 was $>27,000$ exomes in the in-house database at the time of analysis. Only remaining variants
5 present at <0.01 allele frequency in gnomAD (v2.2.1) were retained.
6

7
8 Missense, nonsense, stoploss, splice, splice consensus, frameshift, and indel variants were
9 included in standard evaluation. Synonymous variants outside of the splice consensus
10 sequence, 5-UTR, 3-UTR, non-coding, miRNA, intronic, intergenic, and regulatory variants
11 were only considered if previously published as pathogenic relevant or if indicated by a
12 distinctive phenotype.[13] For variant interpretation, CADD, Polyphen2, and SIFT scores
13 were used for prioritization. Sanger sequencing for all families was performed with the
14 BigDye Terminator v3.1 kit (Life Technologies) according to the manufacturer's instructions
15 and resolved on an ABI3130xl sequencer (Life Technologies). Results were analysed with
16 SeqScape 2.5 (Life Technologies).
17

18 19 *Mouse tissue preparation*

20 Mouse embryos/fetuses were collected at E14.5, E16.5, and on the day of birth (hereafter
21 referred to as E19.5), after matings between C57BL6 mice. For E14.5 and older samples, the
22 whole body was embedded in OCT 4583 medium (Tissue-TEK, Sakura) and frozen on the
23 surface of dry ice. E12.5 embryos were fixed overnight in 4% paraformaldehyde (pH 7.5,
24 w/v) in PBS, cryoprotected by overnight incubation in 20% sucrose (w/v) in PBS, and
25 cryoembedded as described above. Cryosections (Leica CM3050S cryostat) at 10 μm were
26 collected on Superfrost plus slides and stored at -80°C until hybridization. E14.5 samples
27 were sectioned in a frontal plane, whereas other stages were sectioned sagittally.
28
29

30 31 *Probe Synthesis*

32 The *Plxnb2* probe was synthesized from PCR-generated DNA templates kindly provided by
33 the EURExpress consortium (<http://www.eurexpress.org>). The template sequence is provided
34 in the supplementary information. DIG-labeled antisense riboprobe was transcribed in vitro
35 by incubation for 2 h at 37°C using 1 μg of the PCR product, 20 U SP6 RNA polymerase,
36 5X transcription buffer (Promega), 10 X DIG RNA labelling mix (Roche), 0.5 M DTT, 20 U
37 RNase inhibitor (Roche) in a 20 μl volume. The reaction was stopped with 2 μl EDTA (0.2
38 M, pH 8), and RNA was precipitated with 1 μl yeast tRNA (10 mg/ml), 2.5 μl LiCl (4 M) and
39 75 μl absolute ethanol, followed by an incubation for 30 min at -80°C and centrifugation at
40 12,000 rpm (30 min at 4°C). The pellet was washed with 70% ethanol and recentrifuged.
41 The supernatant was discarded and the pellet was allowed to dry. The probe was then diluted
42 in 20 μl sterile H_2O . The quality of the probe was verified by electrophoresis in a 1% agarose
43 gel. If no smear was observed and the size was as expected, the probe was considered to be
44 ready for use. The quantity of RNA was evaluated by a Nanodrop spectrophotometer (ND-
45 1000, Labtech) and adjusted to 150 ng/ μl in hybridization buffer, then stored at -20°C until
46 use.
47
48
49

50 51 *In situ Hybridization*

52 Slides were allowed to thaw to room temperature (RT) for 2 h. Then they were post-fixed on
53 ice in 4% paraformaldehyde (diluted in PBS) for 10 min and rinsed in PBS. The
54 hybridization buffer was composed of 50% deionized formamide, 10% dextran sulfate,
55 1mg/ml yeast tRNA, 1 X Denhardt's solution, and 1 X salt solution (0.195 M NaCl, 5 mM
56 Tris pH 7.2, 5 mM $\text{NaH}_2\text{PO}_4 \cdot \text{H}_2\text{O}$, 5 mM $\text{Na}_2\text{HPO}_4 \cdot 12\text{H}_2\text{O}$, 5 mM EDTA pH 8). The probe
57 was diluted in hybridization buffer at a concentration of 1 $\mu\text{g}/\text{ml}$. The probe mix was
58 denatured by a 10 min incubation at 70°C and placed on ice. 100 μl was applied on each
59 slide and covered by a coverslip. This was allowed to hybridize overnight at 65°C in
60

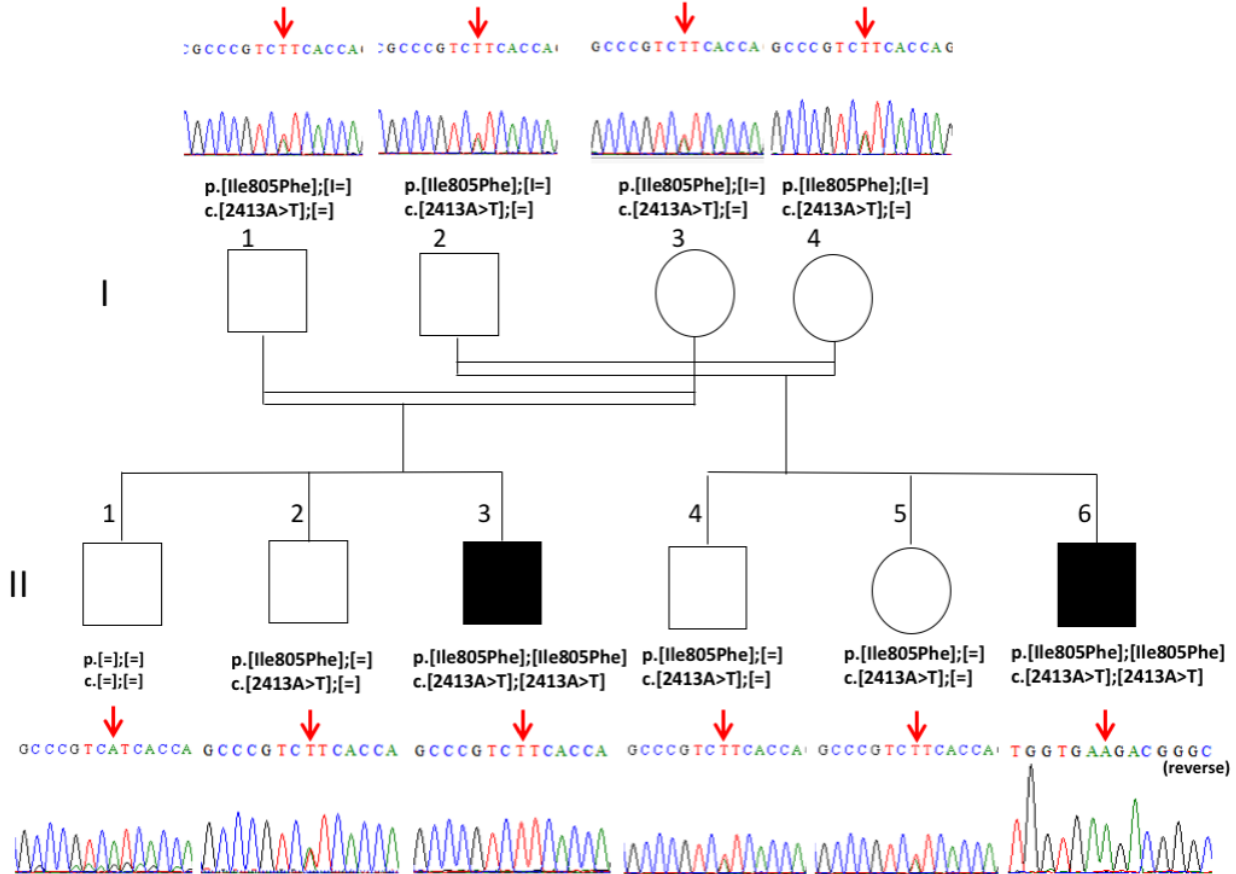
1
2
3 humidified chambers. The slides were then washed twice for 30 min at 65 °C in 1X standard
4 saline citrate (SSC), 50% formamide, 0.1% Tween-20, and twice for 30 min at RT in MABT
5 buffer (1 X MAB (maleic acid buffer): 0.5 M maleic acid (Roche), 0.75 M NaCl pH 7.5,
6 0.1% Tween-20). Probe detection was performed using antibodies and reagents from Roche.
7 Slides were incubated for 1 hr at RT with a blocking solution (20% goat serum, 2% blocking
8 reagent in MABT). The anti-DIG antibody was diluted 1: 2,500 in blocking solution, and 200
9 µl was added to each slide, which were covered by Parafilm and incubated overnight at 4 ° C.
10 Slides were washed 5 times in MABT for 20 min and then twice for 10 min in NTMT buffer
11 (100 mM NaCl, 100 mM Tris-HCl pH 9.5, 50 mM MgCl₂.6H₂O, 0.1% Tween-20). An
12 aliquot of 200 µl of freshly prepared staining solution (3.5 µl nitro-blue tetrazolium chloride
13 (Roche), 3.5 µl 5-bromo-4-chloro-3'indolylphosphate p-toluidine salt (Roche) in NTMT
14 buffer) was placed on each slide, covered by a Parafilm and incubated overnight in the dark
15 at RT. The staining solution was changed every day and when signal was optimal, the slides
16 were rinsed twice for 5 min in NTMT buffer. The slides were further rinsed with PBS and
17 water, allowed to dry overnight, and mounted in Coverquick 2000 mounting medium
18 (Labonord).
19
20
21
22
23
24
25
26
27
28
29
30
31
32
33
34
35
36
37
38
39
40
41
42
43
44
45
46
47
48
49
50
51
52
53
54
55
56
57
58
59
60

Target (GRCh37)	Forward primer (5′)	Reverse primer (3′)	Target (bp)	Primer Identifier (Use)
chr22:507221 18-50722591	TACGGCAAGAATATCG ACAGCAAG	AAATTGGACCCCAGG ATGGTGA	474	Exon 14 (Family 1)
chr22:256008 10-25601544	TGGGAAGATTAACCG GCATCTGG	TGAGGCAGGAGAATG GCATGAAC	735	<i>CRYBB3</i> exon 5 (Family 1)
chr22:507224 28-50722719	GAGGCTGCCCTTGTGA CC	AGAGCTGCCGTCAGT GGT	292	Exon 13 (Family 2)
chr22:507217 64-50722004	ACTTGGAAAGGTGAACT GGACA	CTGTCAGCTGGGTCA GTACC	241	Exon 16 (Family 4)
chr22:507190 90-50719291	TGTGGATGAACTGTAG GGGC	GCGACAAGGACGTGA TGATC	202	Exon 24 (Family 4)
chr22:507150 38-50715798	GTCCCTGGTGGTCTCCT TAC	CAGCACACGAGCAGA GAAAC	761	F5-R7 (Family 5)
chr22:507148 66-50715798	AAGCAGGAGCAGCTCA TACT	CAGCACACGAGCAGA GAAAC	933	F6-R7 (Family 5)
chr22:507169 13-50717351	GATCATTGACCAGGTG TACCG	CACCTTGGACAGGAT GAGG	439	Exon 29 (Family 6)

Supplementary Table 1. Primers used to verify the variants identified in Families 1, 2, 4-6. Primers are for regions of *PLXNB2* unless otherwise stated. Coordinates are for the GRCh37 human reference genome.



Supplementary Figure 1. Family 1: Clinical images of affected individuals. Oral photographs and panoramic radiographs are shown for II:3 and II:6 which illustrate changes over time. The dentitions of both affected individuals are characterised by variable degrees of enamel hypoplasia AI with only a thin layer of enamel present in some places. Crown morphology is atypical in some teeth with striking flattening of normal cusp morphology of the permanent molar teeth evident on radiographs prior to eruption. The radiographic appearances of the dental pulp spaces are within expected limits other than mild taurodontism in some permanent molar teeth. The root morphology is within expected limits. Individual II:6 is shown with bilateral hearing aids.



Supplementary Figure 2. Segregation of the *PLXNB2* variant c.2413A>T, p.(Ile805Phe) identified by exome sequencing of II:3 and II:6.

Family carrying variant and allelic status	Variant (GRCh37)	Transcript (Exon) ENST00000359337.9 / NM_012401.4	Protein	CADD v1.6 GRCh37	REVEL	Polyphen-2 (Hum Var)	SIFT	gnomAD v2.1.1; dbSNP155
1 homozygous	g.50722270T>A	c.2413A>T 14	p.(Ile805Phe)	25.2	0.649	0.97 predicted damaging	0 deleterious	Not present in either
2 homozygous	g.50722576C>T	c.2248G>A 13	p.(Asp750Asn)	23.6	0.159	0.177 benign	0.01 deleterious	Not present; rs1332617247
3 compound heterozygous	g.50728264G>T	c.750C>A 3	p.(Cys250*)	36	N/A	N/A	N/A	Not present in either
3 compound heterozygous	g.50720613C>T	c.3117G>A 19	p.(Thr1039=)	22.7	N/A	N/A	N/A	Not present; rs1234372437
4 compound heterozygous	g.50721841delA	c.2606del 16	p.(Phe869Serfs*45)	17.61	N/A	N/A	N/A	4.024 x10 ⁻⁶ 1/248518; not present
4 compound heterozygous	g.50719182_50719186 delAAAG	c.3982_3986del 24	p.(Phe1328Hisfs*65)	34	N/A	N/A	N/A	Not present in either
5 homozygous	g.50715085_50715672 del	c.5197-337_5310del 34-35	p.(Asp1733_Arg1779del)♦	N/A	N/A	N/A	N/A	N/A
6 homozygous	g.50717063C>T	c.4609G>A 29	p.(Gly1537Ser)	29.1	0.297	0.973 probably damaging	0 deleterious	Not present in either

Supplementary Table 2. Variant interpretation and population frequency data of the *PLXNB2* variants identified in the individuals included in this study. Various pathogenicity prediction scores are included to aid variant interpretation, including Combined Analysis Dependent Depletion (CADD), [14] REVEL, [15] Polyphen-2 [16] and SIFT. [17] The population frequency of each variant in the gnomAD database [4] and its presence or absence in dbSNP155 is also shown. The Genomics England GRCh37 cohort was also checked for these variants, but none were present. Analysis by Franklin (<https://franklin.genoox.com>), showed all variants were classified as VUS (data not shown). Variants are based on genome build GRCh37 and *PLXNB2* transcript ENST00000359337.9, NM_012401.4 and *PLXNB2* protein ENSP00000352288.4, NP_036533.2. ♦Note that splice prediction software predicts the skipping of all of exon 35, despite only partial deletion.

Asp750

1
 2
 3
 4
 5 Zebrafish NVTFYIKDKDTRKIDSTLRVVLNCSVRREDCSLCKNAHKNDSCVWCDT---TKSCIYR 818
 6 Chicken KKLKLSMR--TGKVKIDSKLMVTLYNCSYGRSDCSLCLAAHEDYKCVWCEEDGKPSKCVYE 804
 7 Mouse PLHLYVK--SFGKNIDSKLQVTLYNCSFGRSDCSLCLAADPAYRCVWCRG---QNRVCVYE 793
 8 Human PLHLYVK--SYGKNIDSKLHVTLYNCSFGRSDCSLCRAANPDYRCAWCGG---QSRCVYE 791
 9 Gorilla PLHLYVK--SYGKNIDSKLHVTLYNCSFGRSDCSLCRAANPDYRCAWCGG---QSRCVYE 791
 10 Red deer PLHLYVK--SSGKNVDSRLQVTLYNCSFGRSDCSLCLAADPAYRCVWCSG---QSRCVYE 795
 11 Dog PLHLYVK--SYGKNVDSKLQVTLYNCSFGRSDCSLCLAADPAYKCVWCAG---QGRVCVYE 793
 12 Cat PLHLYVK--SYGKNVDSKLQVTLYNCSFGRSDCSLCLAADPVYKCVWCGG---QSRCVYE 793
 13 Giant panda PLHLYVK--SYDKNVDSKLQVTLYNCSFGRSDCSLCLAADPAYKCVWCAG---QSGCVYE 793
 14 Pig PLHLYVK--SYGKNIDSKLQVTLYNCSFGRSDCSLCLAADPAYKCVWCSG---QSRCVYE 793
 15 Narwhal PLHLYVK--SYGKNIDSKLQVTLYNCSFGRSDCSLCLAADPVYRCVWCSG---QSRCVYA 793
 16 Baleen whale PLHLYVK--SYGKNIDSKLQVTLYNCSFGRSDCSLCLAADPAYQCVWCSG---QSGCVYA 793
 17
 18 : : :: ::* * *.***** *.***** *. *.* * :*:

Ile805

23
 24 Zebrafish SLCDNE-LHQCPPPKITDIDVPRYGPMNGRISVTIKGSNLGIKKEDIKKITVAKVPCIHQP 877
 25 Chicken KLCRAPPTNTCPHPEITRIEPKTGPLDGGILLTIMGSNLGIKAEDVKNITVADKECVFKE 864
 26 Mouse ALCSNV-TSECPPPVITRIQPETGPLGGGILVTIHGSNLGVKADDVKKITVAGQNCAFEP 852
 27 Human ALCN-T-TSECPPPVITRIQPETGPLGGGIRITILGSNLGVQAGDIQRISVAGRNCSEFQP 849
 28 Gorilla ALCN-T-TSECPPPVITRIQPETGPLGGGIRITILGSNLGVQAGDIQRISVAGRNCSEFQP 849
 29 Red deer ALCSNA-TSECPPPVITRIQPETGPLGGGIRITILGSNLGVRADDVVKRVTVAGQNCAFEP 854
 30 Dog ALCSNT-TSECPPPVITRIHPETGPLGGGIRITILGSNLGVTADDVVKRVTVAGQNCAFEP 852
 31 Cat ALCSNA-TSECPPPVITRIHPETGPLGGGIRITILGSNLGVRADDVVKRITVAEQNCVFQF 852
 32 Giant panda ALCSNT-TSECPPPVITRIHPETGPLGGGIRITIVGSNLGVRADVDVGVTVAGQNCVFEP 852
 33 Pig ALCSNA-TSECPPPVITRIHPETGPLGGGIHVTILGSNLGVKADDVTRVTVAGRNCSEFEP 852
 34 Narwhal ALCGNA-TSECPPPVITRIQPETGPLGGGIRVITILGSNLGVRADDVVKRVTVAGRSCAFEP 852
 35 Baleen whale ALCGHA-TSECPPPVITRIQPETGPLGGGIRITILGSDLGVRADDVVKRVTVAGQNCAFEP 852
 36
 37 ** ** * :* * *.**:* * :** **:* : :** * :

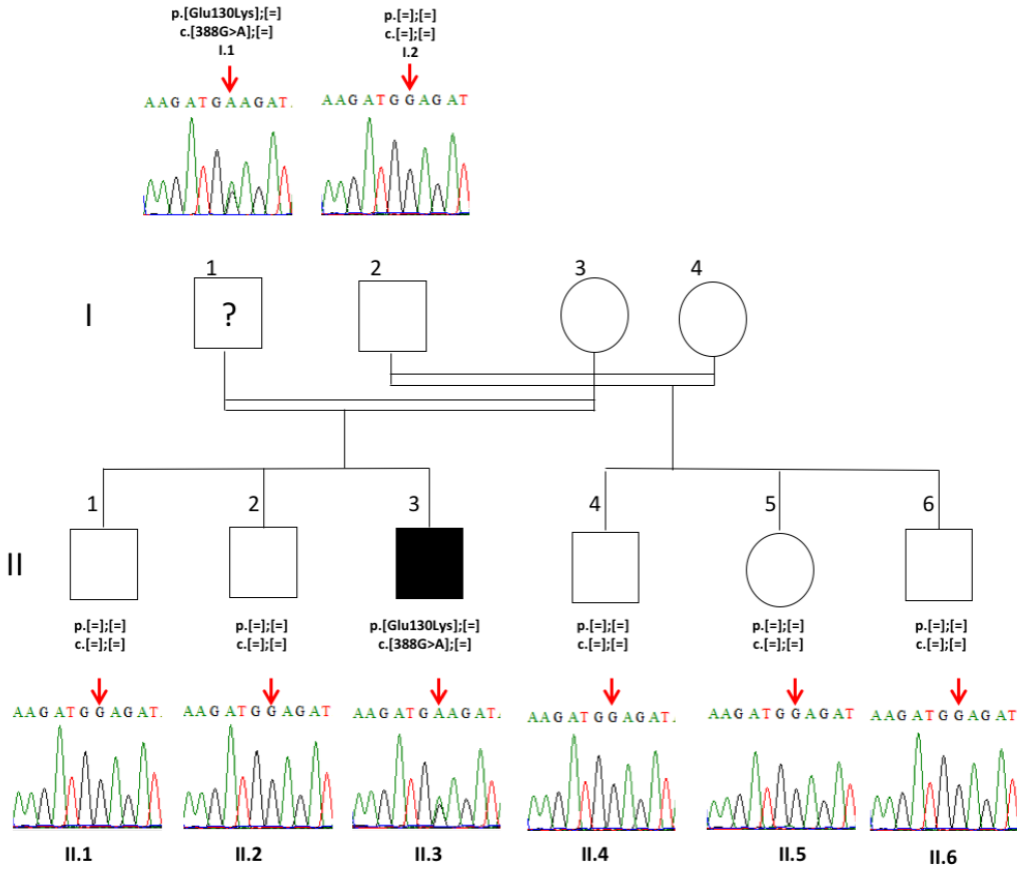
Gly1537

```

1
2
3
4
5 Zebrafish      IEQVYRNLPYSQRPVVDSVALEWRPGSTGQILSDLDLTSQKEGRWKRINTLAHYNVRDGA 1581
6 Chicken      IDQVYRNLPQSQWPKAESVALEWRPGSTAQILSDLDLTSQRDGRWKRINTLMHYNVRDGA 1561
7 Mouse        IDQVYRTQPCSCWPKPDSVVLEWRPGSTAQILSDLDLTSQREGRWKRINTLMHYNVRDGA 1558
8 Human        IDQVYRGQPCSCWPRPDSVVLEWRPGSTAQILSDLDLTSQREGRWKRVNTLMHYNVRDGA 1554
9 Gorilla      IDQVYRGQPCSCWPRPDSVVLEWRPGSTAQILSDLDLTSQREGRWKRVNTLMHYNVRDGA 1554
10 Red Deer     IDQVYRTQPCSRWPKADSVVLEWRPGSTAQILSDLDLTSQREGRWRRVNTLMHYNVRDGA 1559
11 Dog          IDQVYRTQPCSRWPKADSVVLEWRPGSTAQILSDLDLTSQREGRWKRINTLMHYNVRDGA 1557
12 Cat          IDQVYRTQPCSRWPKADSVVLEWRPGSTAQILSDLDLTSQREGRWKRVNTLMHYNVRDGA 1557
13 Giant panda  IDQVYRTQPCSRWPKADSVVLEWRPGSTAQILSDLDLTSQREGRWKRINTLMHYNVRDGA 1557
14 Pig          IDQVYRTQPCSRWPKADSVVLEWRPGSTAQILSDLDLTSQREGRWKRFNTLMHYNVRDGA 1557
15 Narwhal     IDQVYRTQPCSRWPKADSVVLEWRPGSTAQILSDLDLTSQREGRWKRVNTLMHYNVRDGA 1556
16 Baleen whale IDQVYRTQPCSRWPKADSVVLEWRPGSTAQILSDLDLTSQREGRWKRVNTLMHYNVRDGA 1557
17
18 *:*****  * * *  :**.******.******:***:*.*** *****
19
20
21

```

Supplementary Figure 3. Multiple sequence alignment of PLXNB2 sequences from a variety of species to show the evolutionary conservation of the mutated residues suggested to be disease causing. The evolutionary conservation for residues Asp750 (Family 2), Ile805 (Family 1) and Gly1537 (Family 6) and surrounding residues is shown. Disease causing residues are highlighted by a red box. Human (*Homo sapiens*) NP_001363798.1; mouse (*Mus musculus*); gorilla (*Gorilla gorilla gorilla*) XP_030863195.1; pig (*Sus scrofa*) XP_020946968.1; dog (*Canis lupus familiaris*) XP_038535376.1; cat (*Felis catus*) XP_044918511.1; red deer (*Cervus elaphus*) XP_043737305.1; giant panda (*Ailuropoda melanoleuca*) XP_034499687.1; chicken (*Gallus gallus*) XP_046764781.1; narwhal (*Monodon monoceros*) XP_029061558.1; baleen whales (*Balaenoptera musculus*) XP_036721225.1; zebrafish (*Danio rerio*) NP_001155072.1.



Supplementary Figure 4. Segregation of the *CRYBB3* variant c.388G>A, p.(Glu130Lys) identified by exome sequencing of II:3. The variant was inherited from his father (I:1). It is unknown whether I:1 has cataracts.

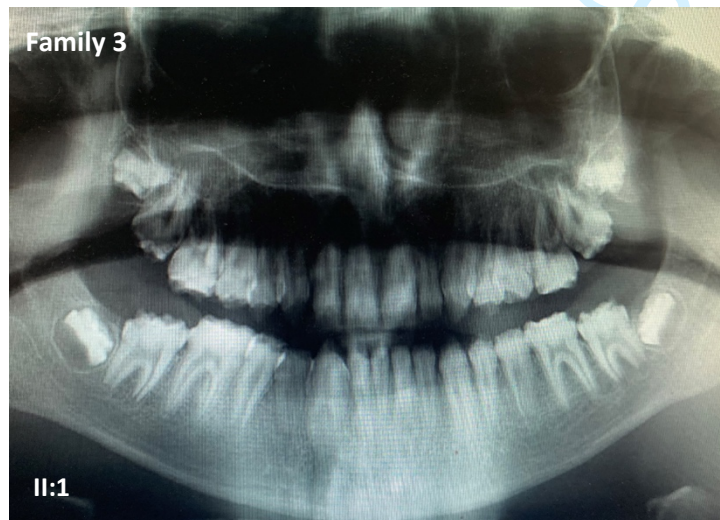
Family	Other genetic findings	Reference sequences
1	chr22:25601247G>A, Homozygous <i>CRYBB3</i> variant c.388G>A, p.(Glu130Lys). Did not segregate with disease for all family members, but was likely responsible for cataract phenotype in some individuals (Supplementary Figure 4).	MANE Select transcript NM_004076.5 (ENST00000215855.7) RefSeq protein NP_004067.1 (ENSP00000215855.2)
2	Chr21:47544826G>A, Homozygous <i>COL6A2</i> variant c.1762G>A:p.(Gly588Ser) [3 hets in gnomAD] segregated with disease for available family members CADDv1.6 score 27.1, in dbSNP (rs139488626), in ClinVar as a benign variant / variant of uncertain significance. However, the published <i>COL6A2</i> disease phenotype is myopathy which was not observed in the affected individual examined. Homozygous variants with CADD>15 were also observed in <i>AQP1/FAM188B</i> (one variant in multiple transcripts) and <i>TRAK1</i> , but variants in these genes have no relevant known disease association and the encoded proteins have no obvious link with symptoms observed in patients, so they were not investigated further.	MANE Select transcript NM_0041849.4 (ENST00000300527.9) RefSeq protein NP_001840.4 (ENSP00000300527.4)
3	No other relevant variants identified. Known and candidate retinal disease genes were specifically checked as this individual was enrolled into a study on inherited retinal disease. The <i>PLXNB2</i> variant was scored highest by pathogenicity prediction software after variant filtering, with no other variants with comparable scores.	
4	Genomes England data had undergone tiering. No other likely causative variants for the phenotypes that the individual was entered into the study under were apparent in Tiers 1-3. The top hit variants for Exomiser were compound heterozygous variants in <i>FLNB</i> (comp het, c.2773G>T, p.(Gly925Cys) [0.1% in gnomAD] and c.124C>T, p.(Arg42*) [absent in gnomAD]). The only other known disease gene with biallelic variants was <i>PKDI</i> (comp het, c.11800G>A, p.(Gly3934Arg) [1 het in gnomAD] and c.872C>T, p.(Ser291Leu) [absent from gnomAD but only present in ENST00000567946, not the MANE Select one]). For both genes, their reported disease phenotype does not fit with the disease phenotype of the affected individual.	<i>FLNB</i> MANE Select transcript NM_001457.4 (ENST00000295956.9) <i>FLNB</i> RefSeq protein NP_001448.2 (ENSP00000295956.5) <i>PKDI</i> MANE Select transcript NM_001009944.3 (ENST00000262304.9) <i>PKDI</i> RefSeq protein NP_001009944.3 (ENSP00000262304.4)
5	Family 5 was identified as having a similar phenotype by the same clinician treating family 4. Homozygous variants with CADD>15 were identified in <i>DENNDH6B</i> , <i>RHBDL1</i> , <i>TSC2</i> , <i>RIMS1</i> , <i>GPBP1</i> , <i>PKDI</i> , <i>SMPD3</i> and <i>COX3</i> . No other rare variants in genes for which variants are known to cause aspects of the phenotype observed in this patient or in candidate genes were identified. The phenotypes expected for these genes, where already known, either do not match the mode of disease inheritance or the phenotype of the affected individual. Parents were noted to be unaffected by disease.	N/A

Family	Other genetic findings	Reference sequences
6	Family 6 was identified through Genematcher, where labs report variants in genes believed to be causative for disease but for which only have one family identified. This flagged an individual with biallelic <i>PLXNB2</i> variants with an overlapping disease phenotype to the other cases. The homozygous variant identified in <i>PLXNB2</i> was scored highest by pathogenicity prediction software after variant filtering, with no other homozygous variants with comparable scores.	N/A

Supplementary Table 3. Details of other genetic findings in affected individuals after variant filtering.



Supplementary Figure 5. Family 2: Clinical images of IV:2 are consistent with hypomineralised AI.



Supplementary Figure 6. Family 3: **II:1** The dental panoramic tomograph (OPT) captures the abnormal dental enamel formation with variable enamel hypoplasia and crown morphology that is especially evident in the unerupted teeth (arrowhead) where the cervical enamel is a more normal morphology compared to the occlusal enamel, which is markedly hypoplastic. These observations are consistent with those for the OPT presented for Family 4 II:1.

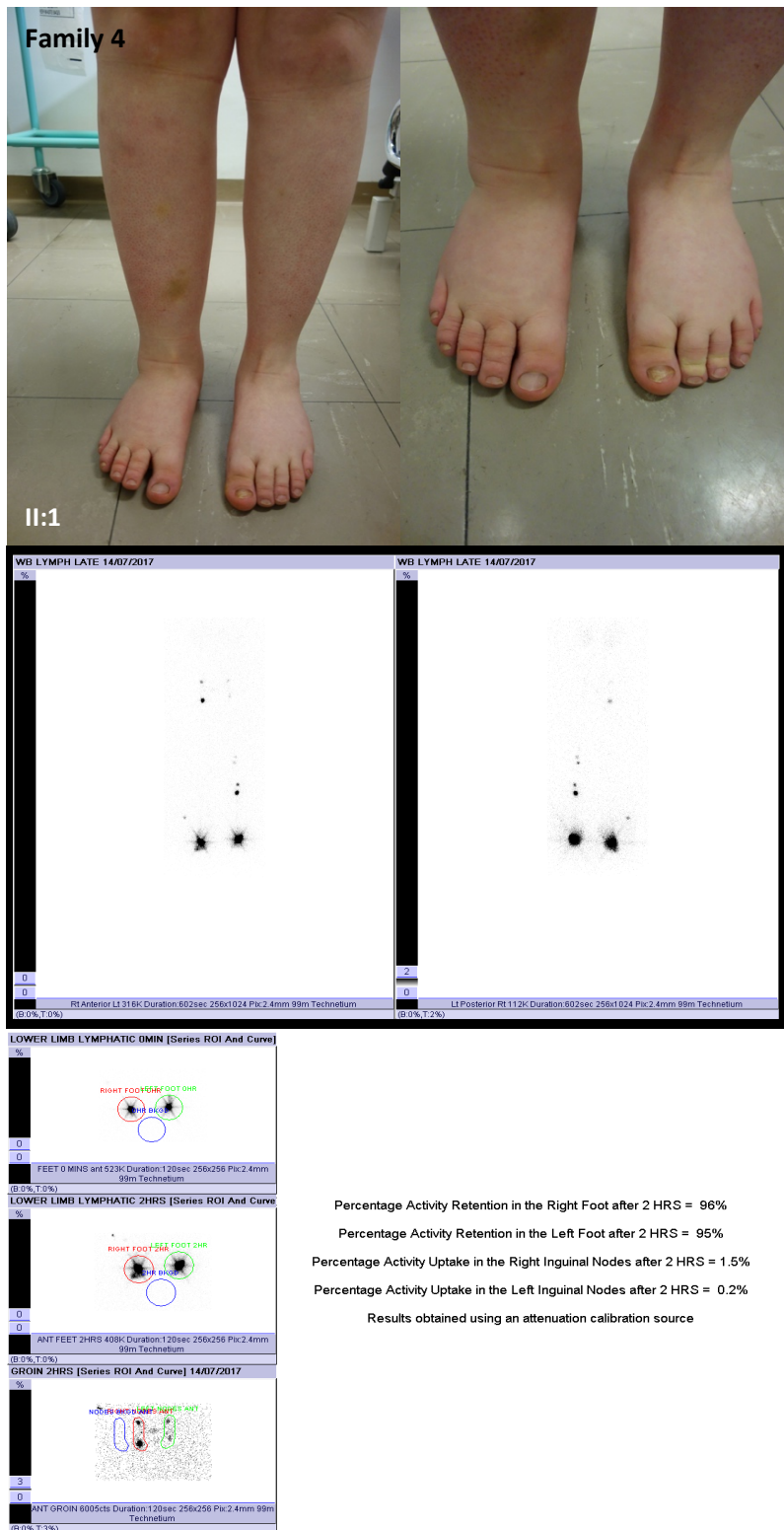
1
2
3
4
5
6
7
8
9
10
11
12
13
14
15
16
17
18
19
20
21
22
23
24
25
26
27
28
29
30
31
32
33
34
35
36
37
38
39
40
41
42
43
44
45
46

Genotype	pos 5'->3' phase strand	confidence	5' exon intron 3'
Wildtype	721 0 +	0.82	GCCCATGACG^GTCAGTCCTG
Mutant	ND		

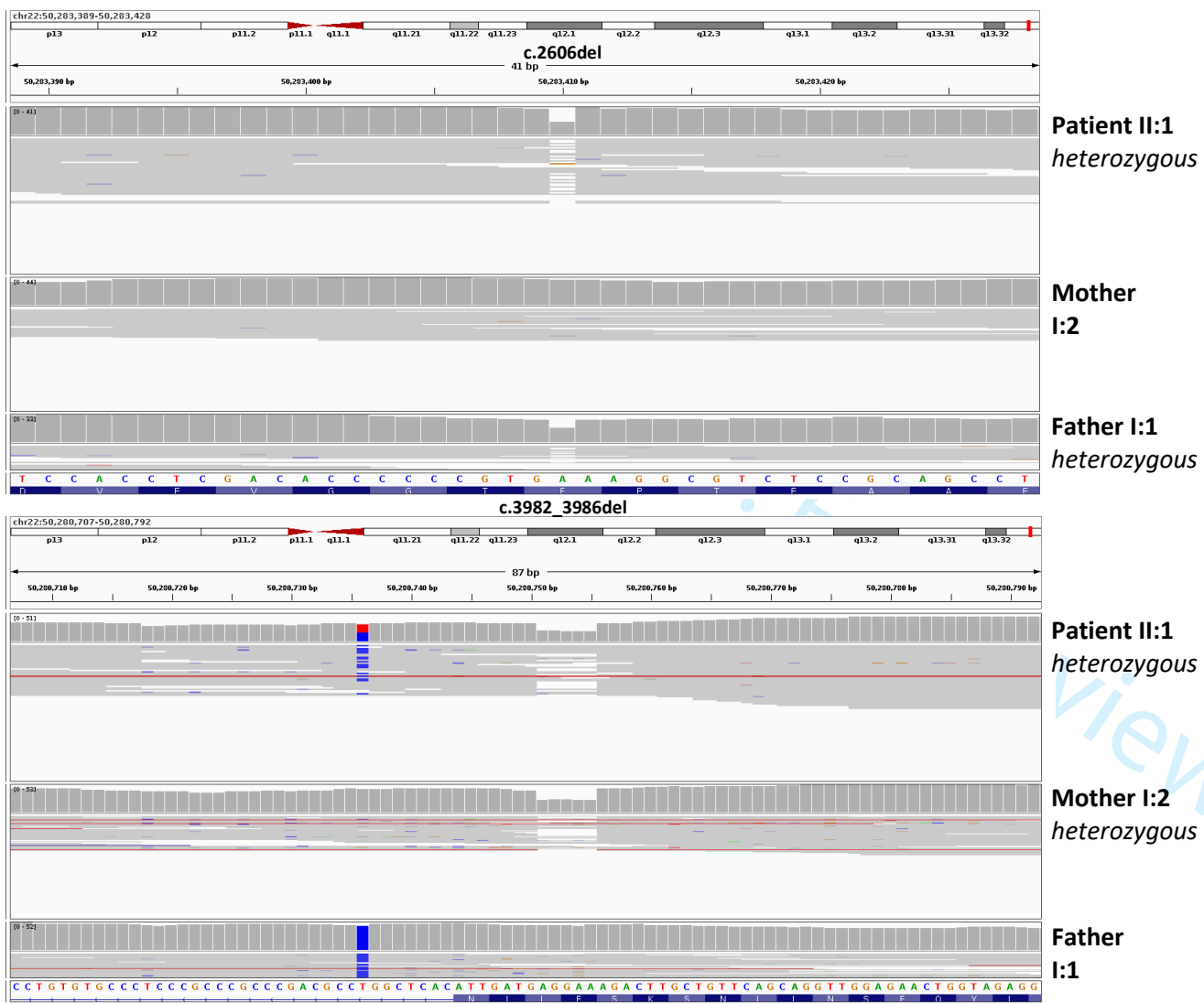
Supplementary Table 4. NetGene2 (v2.4.2) donor splice site predictions for the effect of the variant identified in Family 2. A section spanning the flanking introns and exons was analysed (chr22:50720258-50721332, [based on genome build GRCh37](#), reverse complement), selected results are shown. Wildtype and mutant *PLXNB2* (g.50720613C>T) were investigated. ND not detected.

variant	gene	<input type="checkbox"/> = canonical transcript	<input type="checkbox"/> = non-coding transcript	Δ type	Δ score	pre-mRNA position
22-50282184-C-T UCSC, gnomAD	PLXNB2 (ENSG00000196576.16 / ENST00000359337.9 / NM_001376886.1, NM_001376877.1, NM_001376881.1, NM_001376885.1, NM_001376869.1, NM_001376882.1, NM_001376868.1, NM_001376872.1, NM_001376883.1, NM_001376879.1, NM_012401.4, NM_001376873.1, NM_001376866.1, NM_001376864.1, NM_001376870.1, NM_001376874.1, NM_001376867.1) biotype: protein coding canonical transcript OMIM, GTEx, gnomAD, ClinGen, Ensembl, Decipher, GeneCards	<input type="checkbox"/>	<input type="checkbox"/>	Acceptor Loss	0.00	
		<input type="checkbox"/>	<input type="checkbox"/>	Donor Loss	0.67	0 bp
		<input type="checkbox"/>	<input type="checkbox"/>	Acceptor Gain	0.00	
		<input type="checkbox"/>	<input type="checkbox"/>	Donor Gain	0.00	

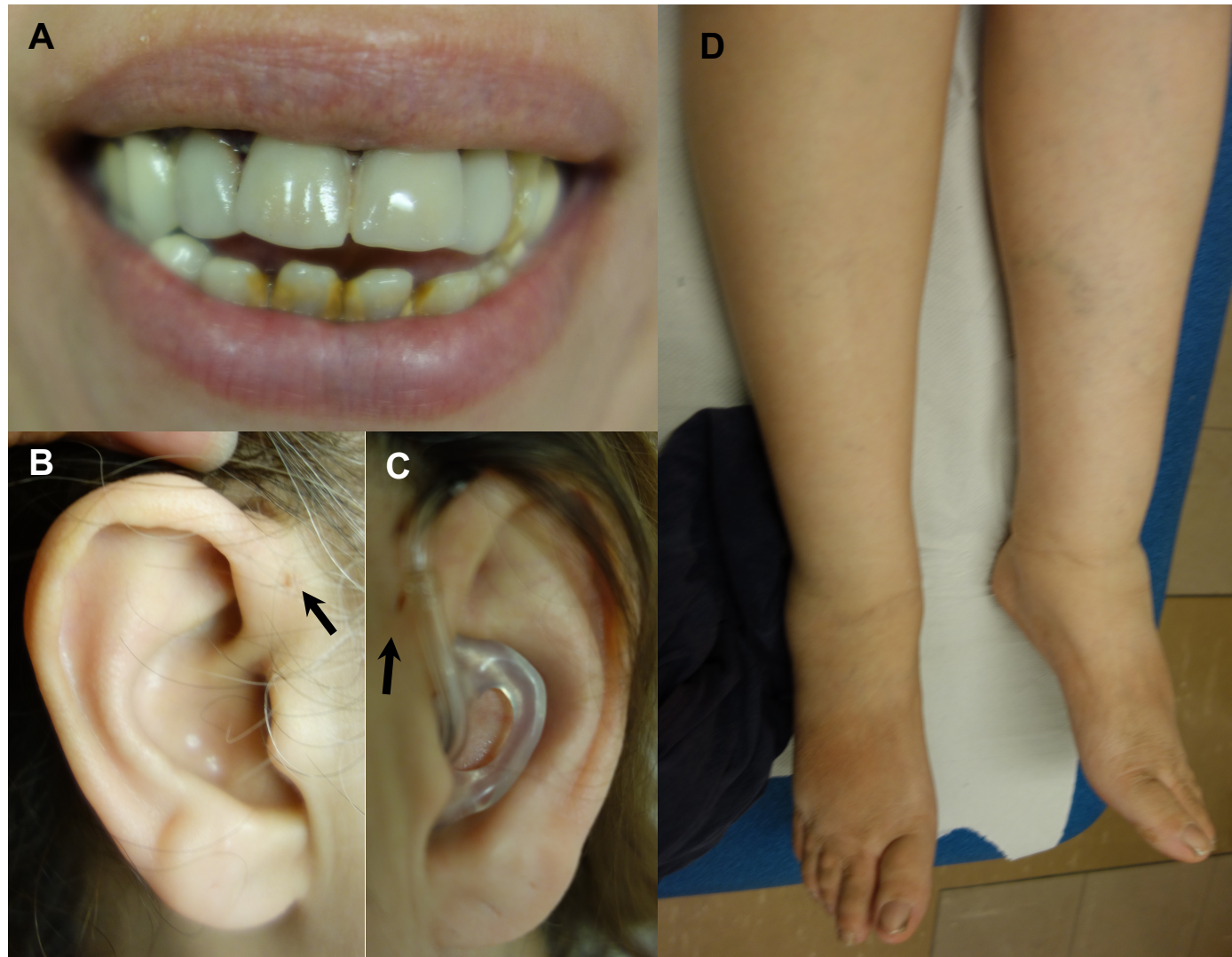
Supplementary Figure 7. SpliceAI predictions for the effect of the variant identified in Family 2. SpliceAI gave the variant a delta score of 0.67 for splice donor loss, which is above the threshold for alterations of splicing of 0.5.



53 **Supplementary Figure 8.** Family 4: Bilateral lower limb lymphoedema in Family 4 II:1.
54 Images show bilateral lower limb lymphoedema. Bilateral lower limb lymphoscintigraphy
55 imaging at 2 hours after injecting radioactive ^{99m}Tc into toe web spaces is also
56 shown. Imaging demonstrates poor uptake into the inguinal lymph nodes with few nodes
57 visualised. The uptake into the inguinal lymph nodes at 2 hours was 1.5% on the right and
58 0.2% on the left, in contrast, normal uptake is $>12\%$. The appearance of popliteal lymph
59 nodes on the left suggesting deep rerouting of the lymphatic tracts.

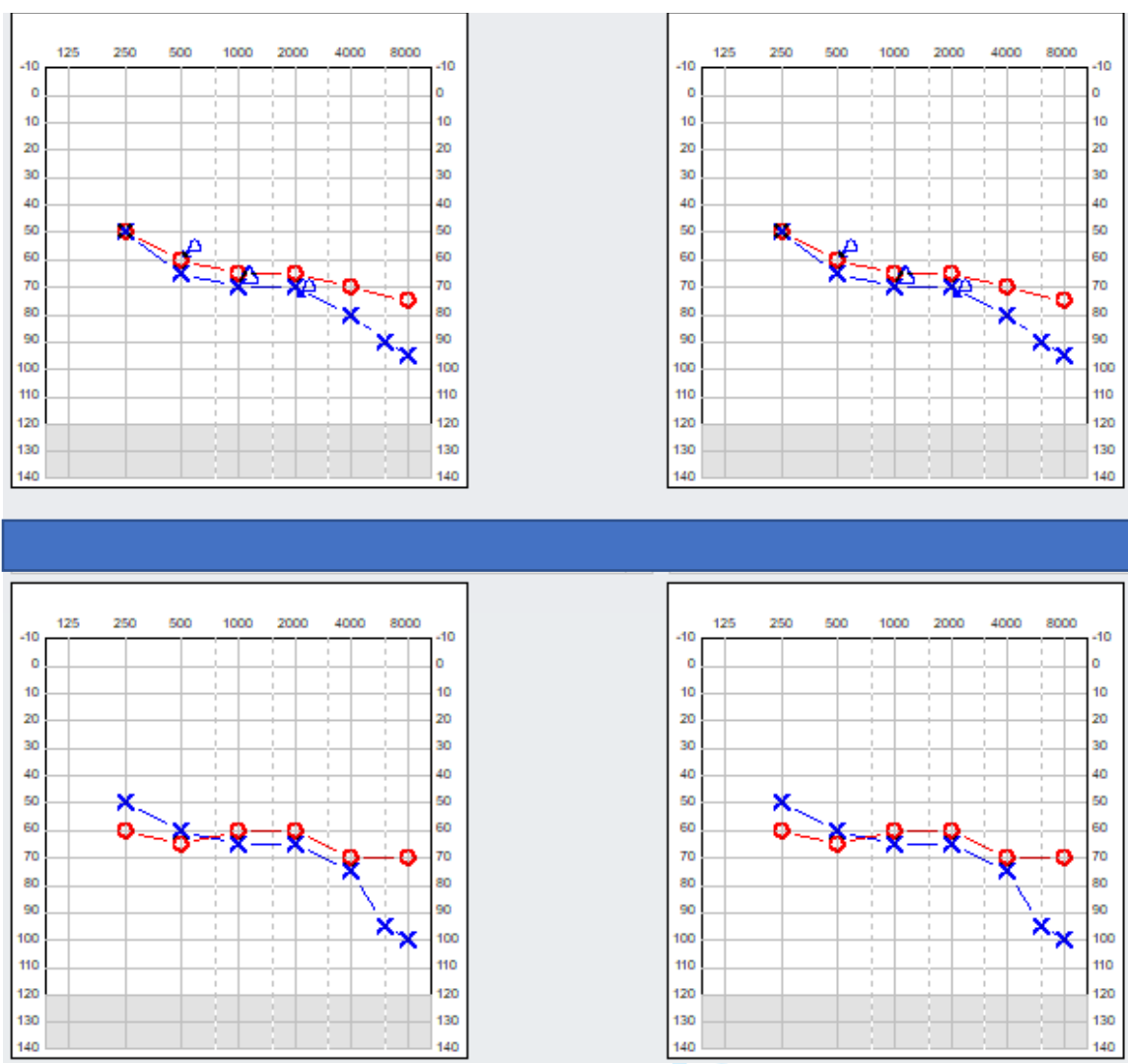


Supplementary Figure 9. IGV images of the variants positions (GRCh38) for individuals from Family 4. IGV traces show c.2606del (upper panel) and c.3982_3986del (lower panel) showing the reduction in read depth relative to the surrounding positions and in comparison to the sequencing of other family members.

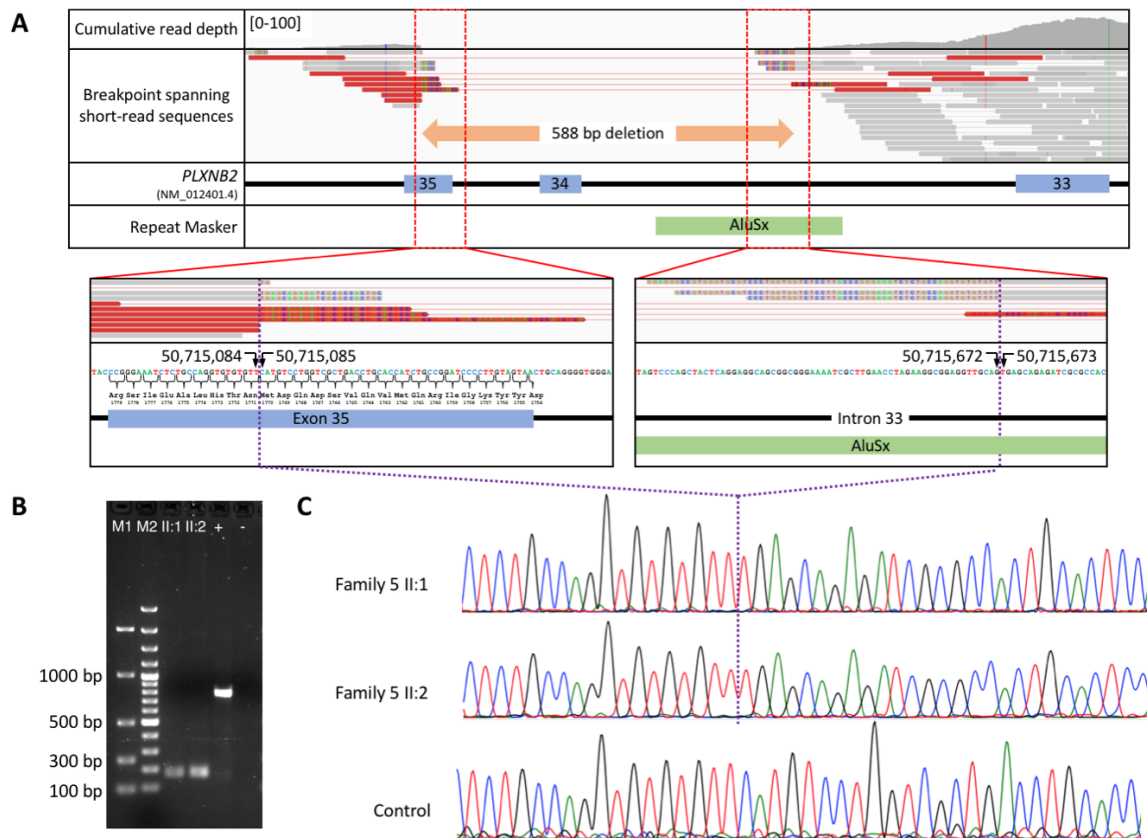


Supplementary Figure 10. Clinical images of Family 5 II:1. A The permanent dentition has been extensively restored and there are calculus deposits on the lower anterior teeth. B and C Periauricular pits are present (blind ended fistulas; arrows). The individual uses a hearing aid. D Bilateral lymphoedema of the lower limbs.

1
2
3
4
5
6
7
8
9
10
11
12
13
14
15
16
17
18
19
20
21
22
23
24
25
26
27
28
29
30
31
32
33
34
35
36
37
38
39
40
41
42
43
44
45
46
47
48
49
50
51
52
53
54
55
56
57
58
59
60



Supplementary Figure 11. Auditory exam history of Family 5 II:1. Results for the left ear (blue) and right ear (red) with headphones are shown for sound frequencies 250-8000 Hz. Results for tests carried out in the past year (top left), one year earlier (top right) and five years earlier are included (both tests shown at the bottom).



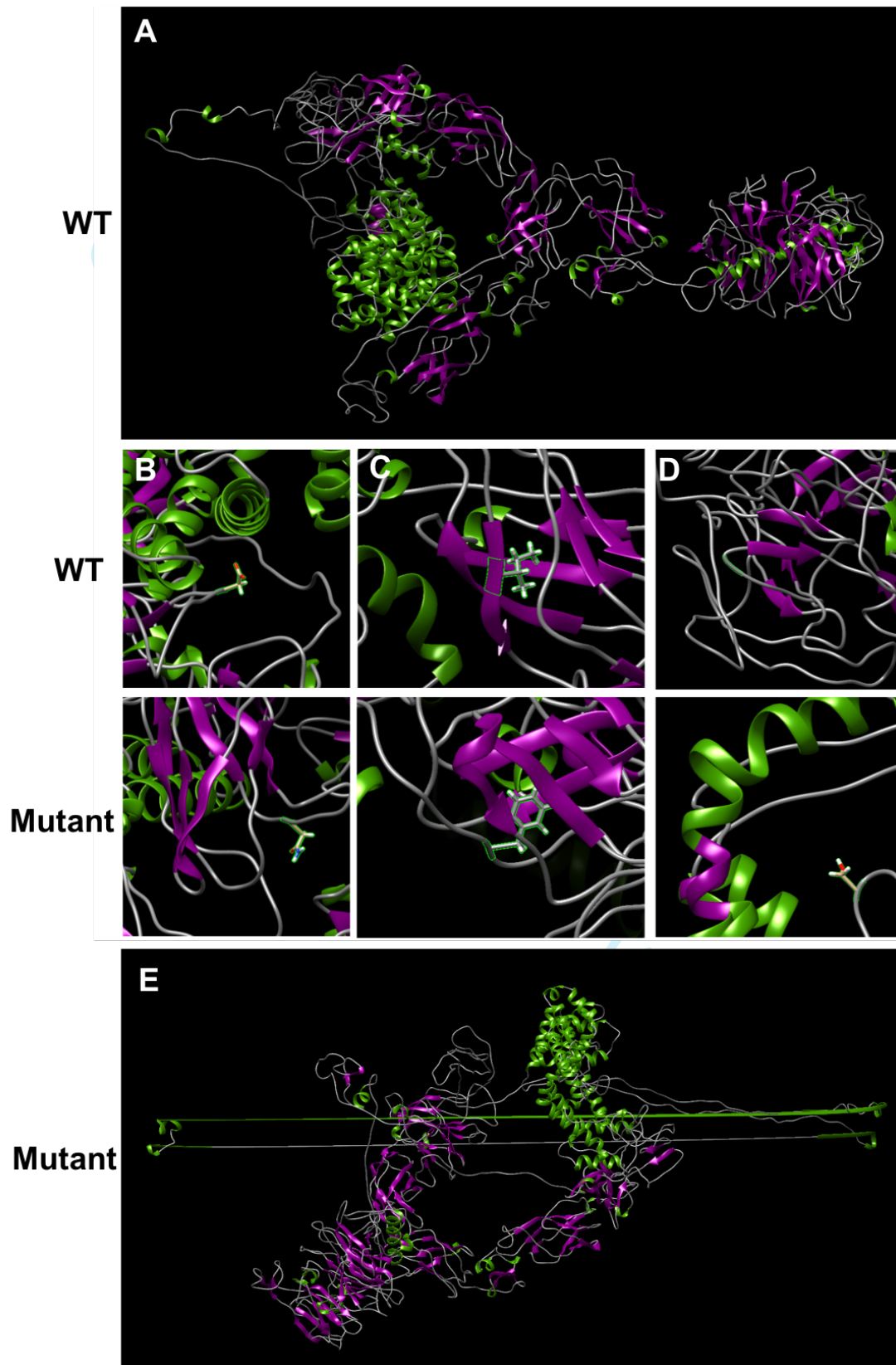
Supplementary Figure 12. Characterisation of the *PLXNB2* deletion in Family 5 by whole exome and Sanger sequencing. **A** Diagram showing the results of short read data analysis. Soft clipped reads revealed the breakpoints to be at chr22:50715085 and chr22:50715672 (based on genome build GRCh37), resulting in the complete deletion of exon 34 and a partial deletion of exon 35, c.5197-337_5310del (NM_012401.4), predicted to result in an in-frame deletion p.(Asp1733_Met1770del) (NP_036533.2), however splicing prediction predicts that the remainder of exon 35 will be skipped, resulting in p.(Asp1733_Arg1779del). **B** Gel image showing products resulting from PCR amplification using primers F5-R7 (Supplementary Table 1). DNA from both II:1 and II:2 but not a control individual produces an approx. 175 bp product when a product of 760 bp is expected. Legend: M1: EasyLadderI (Bioline), M2: 100 bp ladder (Fermentas), + control DNA, - water. **C** Sanger sequencing, using F6-R7 (Supplemental Table 1). confirmed these breakpoint coordinates, revealed that the same deletion was also present in the affected sibling and showed that there were no other alterations around the breakpoints.

Genotype	pos 5'->3' phase strand	confidence	5' exon intron 3'
Wildtype	158 2 +	0.95	TCTGCCTCAG^CTTACCGCTC
Mutant	ND		

Supplementary Table 5. NetGene2 (v2.4.2) acceptor splice site predictions for the effect of the deletion identified in Family 5. A section spanning the flanking introns and exons was analysed (chr22:50,713,408-50,716,325, reverse complement), selected results are shown. Wildtype and mutant *PLXNB2* (g.50715085_50715672del) were investigated. No alternative splice acceptor site was detected. ND not detected.



Supplementary Figure 13. Family 6: Examination of the dentition of III:1 was limited by patient compliance, but extensive post-eruptive enamel changes were clear, with dental caries as a contributory factor.



Supplementary Figure 14. Predicted tertiary structure of PLXNB2 using the I-Tasser-MTD algorithm. **A** Wild-type (WT) protein structure. **B** Comparison of WT with Asp750Asn mutant structure. **C** Comparison of WT with Ile805Phe mutant structure. **D** Comparison of WT with Gly1537Ser mutant structure. **E.** Mutant p.(Asp1733_Arg1779del) protein structure.

1
2
3 CAAAGCAGATGACGTCAAGAAGATAACTGTGGCTGGCCAGAACTGTGCCTTTGA
4 ACCAAGAGGGTACTCCGTATCCACCCGGATTGTGTGTGCAATTGAGGCTTCGGAG
5 ATGCCCTTCACAGGAGGCATTGAGGTGGATGTTAATGGAAAACCTCGGCCATTCA
6 CCGCCACACGTCCAGTTCACCTTATCAACAACCCAGCCTCTCAGTGTGGAGCCAC
7 GACAGGGGCCACAGGCAGGTGGCACCACATTGACCATCAATGGCACTCACCTGG
8 ACACAGGCTCCAAGGAGGATGTGCGGGTGACACTCAATGACGTCCCTTGTGAAG
9 TGACAAAGTTTGGAGCACAGCTACAGTGTGTACAGGTCAACAGTTGGCTCCAG
10 GCCAGGTGACACTAGAAATCTACTATGGGGGCTCCAGAGTGCCAGCCCCGGCA
11 TCTCTTTCACCTACTGCGAGAACCCCATGATACGAGCCTTTGAGCCATTGAGAAG
12 CTTTGTGAGTGGTGGCCGGAGCATCAACGTTACTGGCCAGGGCTTCAGCCTCATC
13 CAGAAGTTTGCCATGGTTGTCATCGCTGAGCCCTTGCGGTCCTGGAGGCGGCGGC
14 GGCGGGAGGCTGGAGCCCTGGAGCGTGTGACGGTCGAGGGGCATGGAGTACGTGT
15 TCTACAACGACACCAAGGTCGTCTTCTTGTCTCCTGCTGTCCCCGAAGAGCCCGA
16 GGCTTACAACCTCACCGTGCTGATA

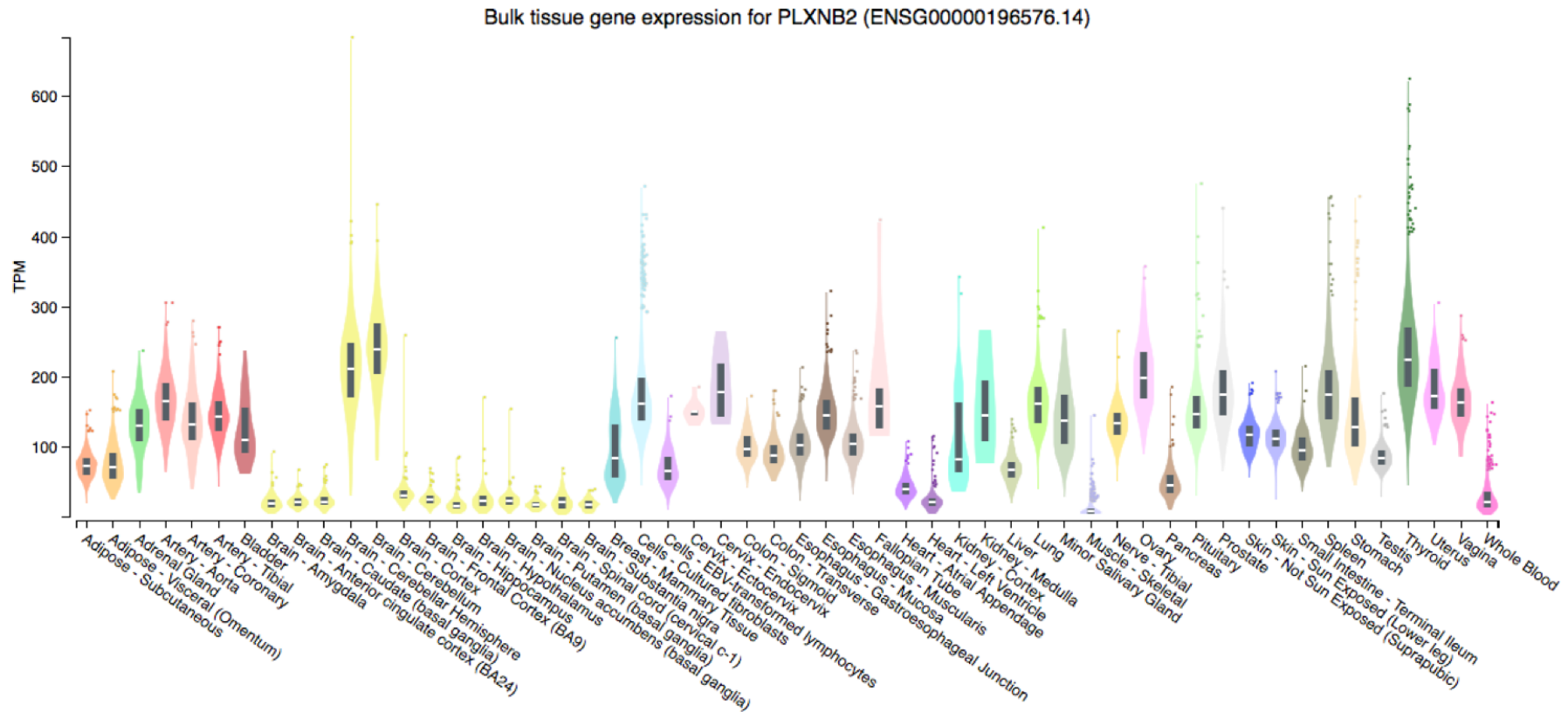
17
18
19
20 **Supplementary Figure 15.** Murine *Plxnb2* template sequence (733 bp) used for in situ
21 hybridization.
22
23
24
25
26
27
28
29
30
31
32
33
34
35
36
37
38
39
40
41
42
43
44
45
46
47
48
49
50
51
52
53
54
55
56
57
58
59
60

Bulk tissue gene expression for *PLXNB2* (ENSG00000196576.14)

Data Source: GTEx Analysis Release V8 (dbGaP Accession phs000424.v8.p2)

Data processing and normalization ⓘ

SUBSET
 SCALE
 TISSUE SORT
 MEDIAN SORT
 OUTLIERS



Supplementary Figure 16. Bulk tissue gene expression for *PLXNB2* from GTEx portal.[18]

References

- 1 Laugel-Haushalter V, Bär S, Schaefer E, *et al.* A New SLC10A7 Homozygous Missense Mutation Responsible for a Milder Phenotype of Skeletal Dysplasia With Amelogenesis Imperfecta. *Front Genet* 2019;10:504. doi:10.3389/fgene.2019.00504
- 2 Backenroth D, Homsy J, Murillo LR, *et al.* CANOES: detecting rare copy number variants from whole exome sequencing data. *Nucleic Acids Res* 2014;42:e97. doi:10.1093/nar/gku345
- 3 Abecasis GR, Auton A, Brooks LD, *et al.* An integrated map of genetic variation from 1,092 human genomes. *Nature* 2012;491:56-65. doi:10.1038/nature11632
- 4 Karczewski KJ, Francioli LC, Tiao G, *et al.* The mutational constraint spectrum quantified from variation in 141,456 humans. *Nature* 2020;581:434-43. doi:10.1038/s41586-020-2308-7
- 5 Yeo G and Burge CB. Maximum entropy modeling of short sequence motifs with applications to RNA splicing signals. *J Comput Biol* 2004;11:377-94. doi:10.1089/1066527041410418
- 6 Reese MG, Eeckman FH, Kulp D, *et al.* Improved splice site detection in Genie. *J Comput Biol* 1997;4:311-23. doi:10.1089/cmb.1997.4.311
- 7 Shapiro MB and Senapathy P. RNA splice junctions of different classes of eukaryotes: sequence statistics and functional implications in gene expression. *Nucleic Acids Res* 1987;15:7155-74.
- 8 Li H and Durbin R. Fast and accurate short read alignment with Burrows-Wheeler transform. *Bioinformatics* 2009;25:1754-60. doi:10.1093/bioinformatics/btp324
- 9 Plagnol V, Curtis J, Epstein M, *et al.* A robust model for read count data in exome sequencing experiments and implications for copy number variant calling. *Bioinformatics* 2012;28:2747-54. doi:10.1093/bioinformatics/bts526
- 10 Turnbull C, Scott RH, Thomas E, *et al.* The 100 000 Genomes Project: bringing whole genome sequencing to the NHS. *Bmj* 2018;361:k1687. doi:10.1136/bmj.k1687

- 1
2
3 11 Conrad DF, Pinto D, Redon R, *et al.* Origins and functional impact of copy number
4 variation in the human genome. *Nature* 2010;464:704-12. doi:10.1038/nature08516
5
6
7 12 Ye K, Guo L, Yang X, *et al.* Split-Read Indel and Structural Variant Calling Using
8 PINDEL. *Methods Mol Biol* 2018;1833:95-105. doi:10.1007/978-1-4939-8666-8_7
9
10
11 13 El-Gazzar A, Mayr JA, Voraberger B, *et al.* A novel cryptic splice site mutation in
12 COL1A2 as a cause of osteogenesis imperfecta. *Bone Rep* 2021;15:101110.
13
14
15
16
17
18
19 14 Rentsch P, Schubach M, Shendure J, *et al.* CADD-Splice-improving genome-wide
20
21
22
23
24
25
26
27 15 Ioannidis NM, Rothstein JH, Pejaver V, *et al.* REVEL: An Ensemble Method for
28
29
30
31
32
33
34
35
36
37 16 Adzhubei IA, Schmidt S, Peshkin L, *et al.* A method and server for predicting damaging
38
39
40
41
42
43
44
45
46
47
48
49
50
51
52
53
54
55
56
57
58
59
60
- 11 Conrad DF, Pinto D, Redon R, *et al.* Origins and functional impact of copy number variation in the human genome. *Nature* 2010;464:704-12. doi:10.1038/nature08516
- 12 Ye K, Guo L, Yang X, *et al.* Split-Read Indel and Structural Variant Calling Using PINDEL. *Methods Mol Biol* 2018;1833:95-105. doi:10.1007/978-1-4939-8666-8_7
- 13 El-Gazzar A, Mayr JA, Voraberger B, *et al.* A novel cryptic splice site mutation in COL1A2 as a cause of osteogenesis imperfecta. *Bone Rep* 2021;15:101110. doi:10.1016/j.bonr.2021.101110
- 14 Rentsch P, Schubach M, Shendure J, *et al.* CADD-Splice-improving genome-wide variant effect prediction using deep learning-derived splice scores. *Genome Med* 2021;13:31. doi:10.1186/s13073-021-00835-9
- 15 Ioannidis NM, Rothstein JH, Pejaver V, *et al.* REVEL: An Ensemble Method for Predicting the Pathogenicity of Rare Missense Variants. *Am J Hum Genet* 2016;99:877-85. doi:10.1016/j.ajhg.2016.08.016
- 16 Adzhubei IA, Schmidt S, Peshkin L, *et al.* A method and server for predicting damaging missense mutations. *Nat Methods* 2010;7:248-9. doi:10.1038/nmeth0410-248
- 17 Ng PC and Henikoff S. SIFT: Predicting amino acid changes that affect protein function. *Nucleic Acids Res* 2003;31:3812-4.
- 18 Melé M, Ferreira PG, Reverter F, *et al.* Human genomics. The human transcriptome across tissues and individuals. *Science* 2015;348:660-5. doi:10.1126/science.aaa0355